Clinical Science (2017) **131** 1261–1281
DOI: 10.1042/CS20160970

Research Article

High serum thrombospondin-1 concentration is associated with slower abdominal aortic aneurysm growth and deficiency of thrombospondin-1 promotes angiotensin II induced aortic aneurysm in mice

Smriti Murali Krishna[1], Sai Wang Seto[1,2], Roby Jose[1], Jiaze Li[1], Joseph Moxon[1], Paula Clancy[1], David J. Crossman[3], Paul Norman[4], Theophilus I. Emeto[1,5] and Jonathan Golledge[1,6]

[1]The Vascular Biology Unit, Queensland Research Centre for Peripheral Vascular Disease, College of Medicine and Dentistry, James Cook University, Townsville, Queensland 4811, Australia; [2]National Institute of Complementary Medicine (NICM), School of Science and Health, University of Western Sydney, Campbelltown, NSW, Australia; [3]Department of Physiology,Faculty of Medical and Health Sciences, Biophysics and Biophotonics Research Group, The University of Auckland, Auckland, New Zealand; [4]School of Surgery, University of Western Australia, Perth, WA 6907, Australia; [5]Public Health and Tropical Medicine, College of Public Health, Medical and Veterinary Sciences, James Cook University, Townsville, Queensland 4811, Australia ; [6]Department of Vascular and Endovascular Surgery, The Townsville Hospital, Townsville, Australia

Correspondence: Jonathan Golledge (jonathan.golledge@jcu.edu.au)

Abdominal aortic aneurysm (AAA) is a common age-related vascular disease characterized by progressive weakening and dilatation of the aortic wall. Thrombospondin-1 (TSP-1; gene Thbs1) is a member of the matricellular protein family important in the control of extracellular matrix (ECM) remodelling. In the present study, the association of serum TSP-1 concentration with AAA progression was assessed in 276 men that underwent repeated ultrasound for a median 5.5 years. AAA growth was negatively correlated with serum TSP-1 concentration (*Spearman's rho* $^{-}$*0.129, P*=0.033). Men with TSP-1 in the highest quartile had a reduced likelihood of AAA growth greater than median during follow-up (OR: 0.40; 95% confidence interval (CI): 0.19–0.84, *P*=0.016, adjusted for other risk factors). Immunohistochemical staining for TSP-1 was reduced in AAA body tissues compared with the relatively normal AAA neck. To further assess the role of TSP-1 in AAA initiation and progression, combined TSP-1 and apolipoprotein deficient ($Thbs1^{-/-}ApoE^{-/-}$, *n*=20) and control mice ($ApoE^{-/-}$, *n*=20) were infused subcutaneously with angiotensin II (AngII) for 28 days. Following AngII infusion, $Thbs1^{-/-}$ $ApoE^{-/-}$ mice had larger AAAs by ultrasound (*P*=0.024) and *ex vivo* morphometry measurement (*P*=0.006). The $Thbs1^{-/-}ApoE^{-/-}$ mice also showed increased elastin filament degradation along with elevated systemic levels and aortic expression of matrix metalloproteinase (MMP)-9. Suprarenal aortic segments and vascular smooth muscle cells (VSMCs) isolated from $Thbs1^{-/-}ApoE^{-/-}$ mice showed reduced collagen 3A1 gene expression. Furthermore, $Thbs1^{-/-}ApoE^{-/-}$ mice had reduced aortic expression of low-density lipoprotein (LDL) receptor-related protein 1. Collectively, findings from the present study suggest that TSP-1 deficiency promotes maladaptive remodelling of the ECM leading to accelerated AAA progression.

Received: 15 December 2016
Revised: 23 March 2017
Accepted: 31 March 2017

Accepted Manuscript Online: 31 March 2017
Version of Record published: 7 June 2017

Introduction

Abdominal aortic aneurysm (AAA) is an important cause of death in older adults due to aortic rupture [1,2]. AAA screening programmes have been introduced in North America, the United Kingdom and

Clinical Science (2017) **131** 1261–1281
DOI: 10.1042/CS20160970

parts of Europe [3]. There has also been an enormous increase in the use of abdominal imaging in most parts of the developed world [4]. As a result in many parts of the world, AAAs are now identified at an early stage when they are small and at a low risk of rupture. Previous randomized trials suggest that asymptomatic small AAAs measuring <55mm should not be treated by surgical repair but rather be monitored by imaging surveillance until they grow to ⩾55mm or become symptomatic [5–8]. However, most small AAAs continue to grow and eventually require surgical repair. Effective medical treatments are needed to limit AAA growth, rupture and requirement for AAA surgery [5–10].

Examination of AAA biopsies from humans and experimental models suggest that chronic aortic wall inflammation and extracellular matrix (ECM) remodelling are important in AAA pathogenesis [1,2]. The thrombospondins (TSPs), are a family of glycoproteins secreted by platelets, macrophages, vascular smooth muscle cells (VSMCs), endothelial cells and fibroblasts [11]. TSP-1 (encoded by the *THBS1* gene) is an endogenous inhibitor of angiogenesis, regulates cell proliferation and plays a crucial role in inflammation [12,13]. TSP-1 modulates VSMC and fibroblast phenotype and preserves the ECM by inhibiting matrix metalloproteinase (MMP) activity [14,15]. TSP-1 interacts with multiple receptors in different cell types and diverse, and at times, paradoxical effects of TSP-1 have been reported [11].

A large body of *in vitro* and *in vivo* data suggests that TSP-1 plays an important role in vascular remodelling by regulating the arterial response to injury [12,16–22]. We previously reported that serum TSP-1 levels were negatively associated with human AAA diagnosis suggesting a possible protective role of TSP-1 against AAA [23]. In support of this theory, we recently reported that a peptide that antagonizes the ability of TSP-1 to activate transforming growth factor β (Tgf-β), promoted AAA growth in an apolipoprotein E (ApoE) deficient ($ApoE^{-/-}$) mouse model in which AAA was induced by angiotensin (Ang) II infusion [24]. Furthermore, TGF-β neutralization with either a rabbit or mouse TGF-β neutralizing antibody enhances AngII-induced aortic rupture and aneurysm formation [25]. In contrast, deficiency of *Thbs1* in C57BL/6 mice (TSP-1 deficient ($Thbs1^{-/-}$)) has been reported to result in protection from AAA induction by peri-aortic application of calcium phosphate ($CaPO_4$) or infusion of elastase [26]. C57BL/6 mice lack concurrent atherosclerosis, which is a usual feature of human AAA [27]. The concurrent presence of atherosclerosis maybe important since TSP-1 has been previously reported to modify atherosclerosis-associated inflammation [28,29]. Given the disparate previous findings regarding the role of TSP-1 in AAA, we performed a combined human and rodent model study to further investigate this. Firstly, we assessed the association of serum TSP-1 concentrations with human AAA growth. Secondly, we assessed the effect of TSP-1 deficiency on abdominal aortic dilatation in a rodent model that incorporated concurrent atherosclerosis ($ApoE^{-/-}$ mice infused with Ang II).

Materials and methods

Patient samples

Sera from participants of the Health In Men Study (HIMS) [30], were used to assess circulating concentrations of TSP-1. Entry criteria included the following: (i) an AAA (defined as maximum aortic diameter ⩾30mm); (ii) a minimum of 3 years ultrasound surveillance and (iii) clinical data and blood samples were available [31,32]. Collection of detailed medical history, clinical examination and blood analysis were carried out on all patients. Identification of cardiovascular risk factors including hypertension, dyslipidaemia, smoking history, diabetes and coronary heart disease (CHD) was as previously defined [33]. The characteristics of the included men are shown in Supplementary Table S1.

Arterial biopsies were obtained from subjects undergoing open surgical AAA repair at The Townsville Hospital, Queensland, Australia. Samples collected from the AAA included full thickness biopsies from the anterior wall of the body (site of maximum aortic dilation) and macroscopically non-dilated proximal neck (site immediately distal to the renal arteries where the aortic diameter was relatively normal). Our previous study suggested that AAA neck samples have a relatively normal morphology with the aortic structure preserved along with minimal inflammation [34]. Paired AAA body and neck biopsies were collected from six patients and a piece of tissue was stored in optimal cutting compound (OCT, ProSciTech) at −80°C for immunohistochemistry (IHC). Approval was obtained from the relevant ethics committees, informed patients' consents were obtained and the study conformed to the guidelines of the Declaration of Helsinki.

Measurement of aortic diameter in patients

AAA growth was assessed using ultrasound-based assessment as reported previously [35]. Maximum anteroposterior and transverse infrarenal aortic diameter were measured by experienced sonographers. Repeated aortic imaging was

performed at the discretion of the local clinician. In general, repeated scans were carried out yearly for 30–44 mm AAAs and every 6 months for 45–50 mm AAAs. Aortic diameter was measured from the outer wall to the outer wall of the artery. The reproducibility of aortic diameter measurements were regularly assessed, with between observer reproducibility coefficients being consistently <4 mm, which we had reported previously [32]. Previous reports published from the group show the reproducibility of the aortic diameter measurements [32,36]. Briefly, to assess intra-rater and inter-rater differences in aortic diameter measurements, ten subjects were selected at intervals of 4 months during the initial screening period and in the follow-up study, at random for assessments. Each man was scanned twice by each observer as well as by a senior vascular sonographer. All scans were performed with the operators blinded to previous aortic diameter measurements. No significant differences were found between observers, with 95% of differences in each of anteroposterior and transverse diameters being <3 mm [32].

AAA induction in mice

$ApoE^{-/-}$ mice were obtained from the Animal Resources Centre, Canning Vale, Western Australia. $Thbs1^{-/-}ApoE^{-/-}$ mice were sourced from the breeding programme of Prof William A. Frazier, Washington University School of Medicine, U.S.A. All animals were housed in the James Cook University (JCU) animal facility with free access to food and water. The temperature in the animal facility was 23 $\pm$ 2°C and the relative humidity was 55 $\pm$ 2%, with a 12 h dark/light cycle. All animal protocols conformed to the Guide for the Care and use of Laboratory Animals by the United States National Institutes of Health and the Australian Code of Practice for the Care and Use of Animals for Scientific Purpose (seventh edition, 2004). Ethical approval was obtained from the local institutional committee prior to commencement of the study.

Twelve-weeks-old male $ApoE^{-/-}$ (n=20) and $Thbs1^{-/-}ApoE^{-/-}$ mice (n=20) were anaesthetized by intraperitoneal (i.p.) injection of ketamine (150 mg/kg) and xylazine (10 mg/kg) and miniosmotic pumps (model 2004, ALZET) delivering 1 μg/kg per min of angiotensin II (AngII, Sigma–Aldrich) were placed subcutaneously as reported previously to administer over 28 days [37–39]. Blood was collected at different time points (baseline, day 14 and 28) into EDTA tubes (BD Vacutainer) to separate platelet-poor plasma. At the end of experiments (14 or 28 days AngII infusion), the mice were killed by CO_2 and blood was collected by cardiac puncture.

Measurement of aortic diameters in mice

Mice were monitored every week by ultrasound sonography using a MyLab 70 VETXV platform (Esaote, Genoa) in B-mode with an LA435 linear transducer (Esaote, Genoa) at an operating frequency of 10 MHz (LA435; Esaote) to provide a sagittal image of the aorta as reported previously [38,40]. Imaging was performed on a constant-temperature table using warm acoustic coupling gel. Maximum suprarenal aortic luminal diameter was measured at peak systole in sagittal images in anterior to posterior plane from the inner to inner aortic wall, using caliper measurements following protocols as previously described by our group [38,39,41]. We have previously demonstrated that ultrasound diameter measurements have good interobserver reproducibility [38,39].

At necropsy, aortas were carefully cleared of peri-aortic fat deposits and perfused with PBS under physiological pressure. Aortas were harvested from mice completing the study protocol or that died during the study. The aortas were excised and placed on a graduated template and digitally photographed (Coolpix 4500, Nikon). The maximum *ex vivo* external aortic diameters of the aortic arch, thoracic aorta (TA), the suprarenal abdominal aorta (suprarenal aorta (SRA)) and the infrarenal aorta (IRA) were measured as previously reported [38,41,42] using Adobe Photoshop software (CS6). Representative portions of aortic segments were dissected and stored in either optimal cutting compound (OCT, ProSciTech) compound or RNA later (Qiagen) for subsequent experiments. Necropsy was performed within 24 h of sudden mouse fatality to confirm aortic rupture as the cause of death.

Non-invasive tail-cuff blood pressure measurements

Tail-cuff measurement of systolic blood pressure (SBP) and heart rate were measured in conscious mice with a non-invasive tail-cuff system (CODA monitor, Kent Scientific, U.S.A.). All animals were acclimatized to the device 2 days before measuring the blood pressure as previously established [42]. All mice were allowed to acclimatize to the restrainer chamber on a warm pad for 10 min in a temperature-controlled room before the measurements and multiple measurements were recorded at each time point, i.e. at baseline (day 0), day 14 and 28 during AngII infusion. Blood pressure and heart rate were measured repeatedly and the measurements were averaged from ten consecutive measurements. Good reproducibility of this technique has been previously established [39,41,42].

Clinical Science (2017) **131** 1261–1281
DOI: 10.1042/CS20160970

Serum and plasma analysis

Sera from AAA patients were assayed to measure creatinine, low-density lipoprotein (LDL), high-density lipoprotein (HDL) and total homocysteine using automated enzymatic assays as previously described [43–45]. Serum high sensitivity C-reactive protein (CRP) concentration was measured by immunophelometry using the BNII analyzer as reported previously (Dade Behring, Milton Keynes, U.K.) [32]. Serum TSP-1, MMP-9, TGF-β1 and plasma interleukin-6 (IL-6) concentrations were measured using previously validated ELISAs according to the manufacturer's instructions (Duoset®; R&D Systems, Minneapolis, Minnesota, U.S.A.) [46].

For the mouse study, platelet-poor plasma were prepared from blood samples taken at the beginning of the study by tail bleeding and end of the study by cardiac puncture. Briefly, platelet-poor plasma was separated by centrifugation of blood at 2000×***g*** at 4°C for 10 min followed by further 10 min centrifugation at 15000×***g*** at 4°C. The plasma samples were snap-frozen in liquid nitrogen and stored at −80°C for subsequent assessments. A multiple analyte mouse inflammation cytometric bead array (CBA, BD Biosciences) was used to quantificatively measure plasma levels of IL-6, IL-10, monocyte chemoattractant protein-1 (MCP-1), interferon-γ (IFN-γ), tumour necrosis factor (TNF) and IL-12p70. Flow cytometry was performed on a CyAn ADP flow cytometer (Beckman Coulter) and CBA data were analysed with FCAP Array software (BD Biosciences), following manufacturer's instructions. Circulating levels of total and active mouse Tgf-β1 (R&D systems) and levels of MMP-9 (R&D systems) were quantified in plasma samples using a commercially available assay according to the manufacturer's instructions. Total nitrate and nitrite (nitric oxide metabolites) were measured in plasma samples by a Nitrate/Nitrite Colorimetric Assay Kit following the manufacturer's protocol (Cayman). Briefly, nitrate was converted into nitrite using nitrate reductase. Subsequent addition of Griess reagents converted nitrite into a deep purple azo compound and the absorbance was measured at 540 nm using an Omega plate reader. We have previously reported this assay to be reproducible [40,42].

Quantification of atherosclerotic lesion area

Presence of aneurysm in the abdominal aorta permitted analysis of atherosclerosis lesions only in the aortic arch, defined as the region from the ascending aorta to 3 mm distal to the subclavian artery. The *en face* Sudan IV staining method is widely used to assess atherosclerotic deposits on the intimal surface [47]. Sudan IV staining was performed in aortic arch segments to assess the atherosclerotic lesion area. The degree of atherosclerosis was quantified and expressed as a percentage of the total luminal surface area following methods described previously. We have shown in multiple studies that this method is highly reproducible [48].

Histopathology

SRA segments stored in OCT (ProSciTech) from each mice group were selected using a random number generator and cut into 6-μm-thick sections. The adjacent sections were stained with haematoxylin and eosin (H&E, ProSciTech) and mounted in Entellan mounting medium (Electron Microscopy Sciences, U.S.A.). Aortic sections were also processed for Elastin Van Gieson (EVG) staining (Polysciences, Inc) for elastin and Picrosirius staining (Polysciences, Inc) for collagen. The stained H&E and EVG sections were photographed using a Nikon Eclipse 50i microscope fitted with a CCD camera (DSF*i*1) and digital images captured into a PC supported with NIS Elements (version F2.30).

Elastin filament fragmentation in each field was recorded under 40× magnification from two to three aorta sections from each mouse. Elastin fragmentation was graded for quantitative evaluation as reported previously according to the following criteria: 1–no elastin breaks, 2–mild fragmentation, 3–moderate to severe and 4–severe elastin filament fragmentation. We have shown previously that this grading method is highly reproducible [49,50]. Images were obtained under polarization microscope (Zeiss AxioVision) to assess collagen content and expressed as percentage of stained area of the total section area under bright field. Sections were photographed with identical exposure setting for each section. The percentage of birefringence was determined for four to five fields of at least three sections from each mouse (n=6/group), and the mean value was calculated for each region as described previously [24].

To localize cells undergoing nuclear DNA fragmentation, *in situ* terminal deoxynucleotidyl transferase (TdT) mediated dUTP nick-end labelling (TUNEL) was performed using an *in situ* apoptosis kit specially developed for vascular tissues (VasoTACS, Trevigen). The cryostat sections (6μm) were processed for the TUNEL assay as described previously [50,51] and both positive and negative control slides were processed at the same time (n=6). The presence of apoptotic cells was identified as dark nuclear staining with the distinctive morphological appearance associated with cell shrinkage and chromatin condensation (apoptotic cells) or cytoplasmic fragments with or without condensed chromatin (apoptotic bodies). The images were captured at 400× magnification, and percentage of positive staining area was calculated by dividing the positive staining area by the total area of the region selected. For each

region of interest, a spot check was performed by visually counting the cells and avoiding necrotic areas. All histological evaluations were done in a blinded fashion in at least three to four sections per sample (intra-assay coefficient of variation =2.97%, n=5 [50]).

IHC

Aneurysmal and adjacent non-aneurysmal human aortic samples were obtained during surgery from six patients undergoing AAA repair. Removal of these tissues was accomplished as a part of the normal operative procedure, in which both aneurysm and adjacent non-aneurysmal segments were trimmed in preparation for graft anastomosis and stored in OCT compound. Serial cryostat sections (6 μM) were cut from each tissue sample on to silane-coated slides (ProSciTech). The sections were air dried, fixed in acetone for 10 min at −20°C, air dried and processed for IHC as described previously [24]. Human aortic sample sections were stained with a TSP-1 antibody (1:200; Santa Cruz Biotechnology, U.S.A.).

Randomly selected $ApoE^{-/-}$ and $Thbs1^{-/-}ApoE^{-/-}$ suprarenal aortic segments were stored in OCT compound (ProSciTech). Serial cryostat sections (6 μM) were cut from each tissue sample on to silane-coated slides (ProSciTech) and sections were air dried, fixed in acetone for 10 min at −20°C, air dried and processed for IHC as described previously [38]. Briefly, the sections were rehydrated with PBS before being incubated in 3% H_2O_2/0.1% sodium azide/PBS to block endogenous peroxidase. Slides were then incubated in 2% normal goat serum (Vector Laboratories) in PBS and endogenous avidin and biotin blocked using Avidin/Biotin Blocking Kit (Vector Laboratories), then incubated with primary antibody anti-monocyte and macrophage antibody (MOMA-2, 1:500; ab33451) overnight at 4°C. The secondary antibody used was biotinylated anti-rat IgG (BA-9400, 1:500 dilution, Vector). Slides were incubated in the peroxidase substrate 3,3′-diamminobenzidine (ImmPACT DAB, Vector), counterstained in Mayer's Haematoxylin, dehydrated, cleared in xylene and mounted in Entellan mounting medium (Electron Microscopy Sciences). Sections were stained simultaneously, using identical reagents and incubation times. Specimens incubated with non-relevant isotype-matched monoclonal negative controls for animal studies and no primary antibody for human specimens served as negative controls. Digital images of the stained sections were photographed using the Nikon microscope (Nikon Eclipse 50i) as mentioned in the previous section and staining was quantified by image analysis. Image analysis was performed on digital-tiff images captured into a PC supported with image analysis software (NIS Elements, version F2.30) and quantified as described previously by our group [38,39].

In situ zymography

Cryostat sections (6 μM) obtained from suprarenal aortic segments embedded in OCT underwent *in situ* zymography using MMP fluorogenic substrate DQ–gelatin–FITC (20 μg/ml, Invitrogen). In brief, frozen aortic tissues were pre-incubated in water at 37°C for 40 min, and then overlaid with a fluorogenic substrate DQ gelatin (20 μg/ml, Invitrogen) diluted 1:100 in the buffer supplied by the manufacturer, for 40 min at 37°C. The sections were washed with PBS and fixed in 4% paraformaldehyde (PFA, Sigma), at room temperature for 15 min. The sections were washed and allowed to dry prior to placement of a coverslip (Vector Labs). The signal was observed through an immunofluorescent microscope (Zeiss AxioVision) and the proteolytic activity (combined gelatinase activity of MMP-2 and MMP-9) was detected as bright green fluorescence (530 nm). The specificity of the reactions was examined using global chemical MMP inhibitors 1, 10-phenanthroline (20 mm/l, Molecular Probes), and EDTA (10 mmol/l) was used to define non-specific fluorescence. Digital images were analysed in a blinded manner and presented as percentage area showing gelatinase activity in relation to the total area of the section selected.

Confocal microscopy

Whole thickness suprarenal aortic biopsies from saline infused $ApoE^{-/-}$ (n=3) and AngII-infused $ApoE^{-/-}$ mice (n=3), were fixed and processed for confocal microscopy as previously described [52]. Tissues were probed with rabbit anti-LDL receptor-related protein 1 (LRP1, 1:200, ab92544) overnight at 4°C, followed by goat anti-rabbit Alexa Fluor® 568 and phalloidin Alexa Fluor® 488 (Life Technologies) for 2 h at room temperature. A Zeiss LSM 710 inverted confocal microscope was used to image sections with a 10× lens (0.4 NA) and 63× (1.4 NA) lens with the pinhole set to 1 airy unit. The lasers had wave length of 488 and 568 nm and the pixel resolution was 0.28 μm per pixel for 10× lens and 0.082 μm per pixel for 63× lens.

Clinical Science (2017) **131** 1261–1281
DOI: 10.1042/CS20160970

Isolation of VSMCs

Primary VSMCs were isolated from the aortas of 8–12-week-old male $Thbs1^{-/-}ApoE^{-/-}$ (n=6) and littermate $ApoE^{-/-}$ mice (n=6), subjected to subcutaneous infusion of AngII for 14 days as mentioned in the previous section. All mice were anaesthetized with a mixture of ketamine/xylazine (100 and 10 mg/kg body weight respectively) and killed by CO_2 asphyxiation. Briefly, adhering fat and connective tissue were removed by blunt dissection from the aorta. The aorta was harvested under dissection microscope magnification, and placed in ice-cold culture medium (DMEM with 10% FBS, 100 U/ml penicillin, 100 mg/ml streptomycin and 2 mM glutamine; Gibco) [53]. The endothelial layer was denuded with a sterile cotton bud and the adventitia was excised with microsurgical instruments. The aorta was cut into 1-mm fragments and incubated with 1 mg/ml collagenase type I (Worthington, Lakewood, NJ) and 0.125 mg/ml elastase type III (Worthington, Lakewood, NJ) at 37°C for 4 h. Cell suspension were centrifuged at 1500 ***g*** for 10 min at 4°C and cell pellets were resuspended in DMEM containing 10% FBS. The mixture was then aliquoted into 25 cm^2 culture flasks and allowed to grow at 37°C and 5% CO_2 with medium changed every 3 days. Primary cultures without passages were harvested at day 11 for analysis to minimize contamination with other cell types.

mRNA analysis by quantitative real-time PCR

Total RNA was isolated from suprarenal aortic segments and VSMCs derived from mice. Eight SRA segments stored in RNA Later (Qiagen) were selected from each group using random number generators for gene expression analysis by quantitative real-time PCR (qRT-PCR). Total RNA was isolated using an RNeasy Mini kit (Qiagen) according to manufacturer's instructions and quantified spectrophotometrically using Nanodrop 2000. Total RNA (20 ng) was used for qRT-PCR using QuantiTect SYBR Green one-step RT-PCR assay (Qiagen) as per manufacturer's instructions. qPCR was performed to evaluate gene expression for the samples using RT^2 qPCR Primer Assay for Mouse (Qiagen) designed for collagen type 1A1 (*Col1A1;* PPM03845F), collagen type 3A1 (*Col3A1;* PPM04784B), *Lrp1* (PPM05653F), *Mmp-9* and glyceraldehyde-3-phosphate dehydrogenase (*Gapdh;* QT01658692). GAPDH was chosen as the housekeeping gene, since analysis showed its expression to be stable across the samples. PCR reactions were run in duplicate in the RotorGeneQ (Qiagen). For each gene of interest, the relative expression in each sample was calculated by using the concentration-Ct-standard curve method and normalized to the average expression of *GAPDH* [41].

Western blotting

SRA segments (n=6/group) stored in OCT compound (ProSciTech) were randomly selected using a random number generator and were homogenized in RIPA buffer (Cell Signaling) in the presence of protease inhibitors (Roche) to obtain total protein extracts. Protein concentrations were determined using a Bradford Protein Assay Kit following manufacturer's instructions (Bio–Rad). Samples (25 μg of protein per lane) were loaded on to a SDS/PAGE (10% gel). After electrophoresis (110 V, 90 min), the separated proteins were transferred (15 mA, 60 min) on to a PVDF membrane (Bio–Rad) and were blocked with 5% non-fat dry milk (5%) that was used for 60 min to block non-specific sites, and the blots were then incubated with anti-total-*Smad2/3* antibody (1:1000, sc-11769; Santa Cruz Biotechnology), anti-p-*Smad2/3* antibody (1:1000, sc-8332; Santa Cruz Biotechnology), anti-total-*Akt* antibody (1:1000, SAB4500797, Sigma–Aldrich) and anti-p-*Akt* antibody (1:1000, 07-1643; Sigma–Aldrich) overnight at 4°C. Anti-rabbit HRP–conjugated IgG (1:1000, DakoCytomation) or anti-goat HRP–conjugated IgG (1:1000, DakoCytomation), were used to detect the binding of its corresponding antibody. The protein expression was estimated with Western Lightning Chemiluminescence Reagent Plus (PerkinElmer Life Sciences) and quantified by Quantity One software (version 4.6.7, Bio–Rad).

Statistical analysis

The association of TSP-1 with AAA growth (assessed by ultrasound measurements) was analysed using Spearman's rho correlation coefficient and multiple logistic regression. Data from mouse studies were analysed using GraphPad Prism (version 6). Parametric or non-parametric tests were applied appropriate to the distribution of data. Accordingly, aortic end point data for maximum diameter and mRNA expressions were compared using unpaired t test or Mann–Whitney U test and expressed as mean ± S.E.M. or median and interquartile range (IQR) respectively. Comparison of data obtained as a function of time was performed using repeated measures two-way ANOVA with Bonferroni post hoc applied for multiple testing, i.e. blood pressure and ultrasound measurement of the SRA diameter. Categorical data were compared using Fisher's exact tests. Kaplan–Meier survival curves were analysed using log-rank (Mantel–Cox) test. In all cases, statistical significance was assumed at $P<0.05$.

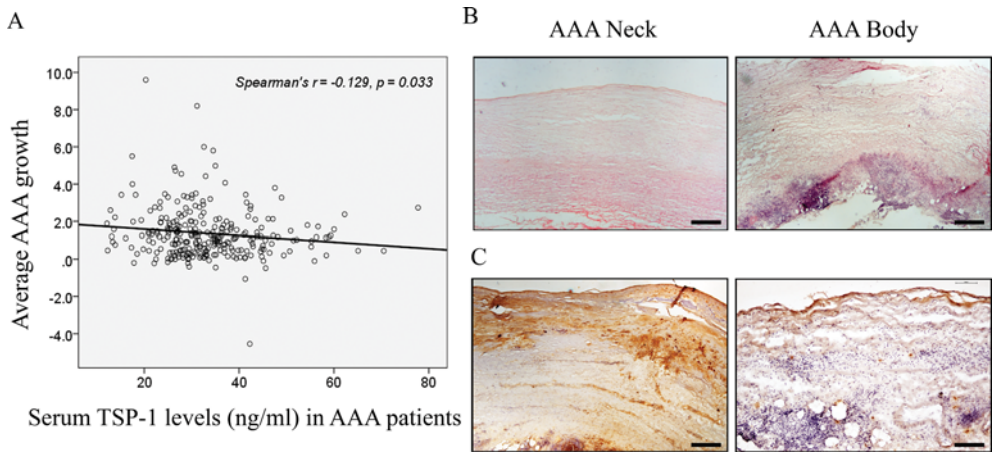

Figure 1. Serum TSP-1 concentration was negatively correlated with AAA growth and down-regulated in AAA samples

(**A**) Spearman's correlation graph showing inverse correlation between average AAA growth and serum TSP1 levels in AAA patients (n=276). (**B**) Representative serial cryostat sections of full-thickness human AAA tissues showing H&E staining. The section of the AAA body shows inflammatory cells and a disrupted medial layer. (**C**) Representative serial paraffin sections of full-thickness human AAA tissues with immunostaining (brown) for TSP-1. The staining for TSP-1 was found to be intense in the biopsy from the proximal AAA neck compared with weak staining in AAA body section. Low power (×100) photomicrographs. Scale bar =50 μm.

Results

High serum TSP-1 concentration was associated with slower AAA growth, and expression of TSP-1 was low in samples from the main body of human AAA

The serum concentration of TSP-1 was assessed in a subset of the participants of the HIMS and details of the men included in the study are given in the Supplementary Table S1 [30]. Men with AAAs (n=276) measuring a median (IQR) initial diameter of 32.9 mm (IQR: 31.0–36.1 mm) were followed up for a median of 5.5 years (IQR: 5–6 years) with a median of 7 (IQR: 6–7) ultrasound scans. Median AAA growth as measured by ultrasound was 1.1 mm per year (IQR: 0.5–1.9) and AAA growth was weakly and negatively correlated with serum TSP-1 concentration (*Spearman's rho* $^{-}$*0.129, P*=0.033, n=276) (Figure 1A).

AAA patients were grouped into four quartiles based on the serum levels of TSP-1. Subsequently, men with serum TSP-1 concentrations in quartiles 2–4 were compared with subjects who had serum TSP-1 in the lowest quartile. After adjusting for risk factors previously reported to be associated with AAA growth (including initial AAA diameter, diabetes, CHD, smoking and statin prescription) men with TSP-1 in the highest quartile had a reduced likelihood of AAA growth greater than median during follow-up. Men with serum TSP-1 levels in the fourth quartile (>38.36 ng/ml) were less likely to have AAA growth greater than median than those with TSP-1 in the first quartile (OR: 0.40; 95% confidence interval (CI): 0.19–0.84, P=0.016) (Table 1). TSP-1 concentrations were not associated with serum concentrations of creatinine, HDL, high sensitivity CRP (hs-CRP), homocysteine and plasma IL-6 (Supplementary Tables S2 and S3). Circulating concentrations of TSP-1 were positively correlated with circulating concentrations of TGF-β1, MMP-9 and LDL (Supplementary Tables S2 and S3).

To assess the expression of TSP-1 in human AAA samples, we performed IHC using samples taken from the site of main aortic dilatation (the AAA body) and the relatively non-dilated neck of the AAA. We have previously reported that samples from the AAA neck have relatively preserved aortic structure and minimal inflammation [34]. Histopathological analysis showed that AAA body sections had evidence of marked inflammation and medial layer destruction, while biopsies of the proximal non-dilated AAA neck showed minimal inflammation and limited medial layer destruction, as previously reported (Figure 1B) [34]. TSP-1 protein expression was relatively down-regulated in AAA body compared with AAA neck (Figure 1C).

Clinical Science (2017) **131** 1261–1281
DOI: 10.1042/CS20160970

Table 1 Logistic regression model assessing the association between AAA growth greater than median and serum TSP-1 quartiles

Characteristics	OR	95% CI	*P-value*
Serum TSP-1 (ng/ml)*			
<26.58 (*n*=69)	1	*Reference group*	
26.58–31.62 (*n*=68)	0.72	0.34–1.51	0.378
31.62–38.36 (*n*=70)	0.50	0.24–1.04	0.063
>38.36 (*n*= 69)	0.40	0.19–0.84	**0.016**
Initial AAA diameter >32.9 mm†	3.39	2.01–5.71	**<0.001**
Statin prescription	1.31	0.77–2.22	0.326
CHD	0.73	0.43–1.26	0.265
Ever-smoker	0.70	0.34–1.43	0.330
Diabetes mellitus	0.24	0.10–0.59	**0.002**

For nominal variables, the comparisons are to subjects without the risk factor. Staistically significant *P*-values are show in bold.
*Men with serum TSP-1 concentrations in the top, second and third quartiles were compared with subjects who had serum TSP-1 in the lowest quartile.
†Approximately median value. Abbreviation: *n*, number.

Table 2 Cardiovascular, biochemical and cellular effects of AngII infusion in *ApoE*$^{-/-}$ and *Thbs1*$^{-/-}$ *ApoE*$^{-/-}$ mice at day 28

Parameters assessed	*ApoE*$^{-/-}$ (*n*=13)	*Thbs1*$^{-/-}$*ApoE*$^{-/-}$ (*n*=16)	*P*-value
Ultrasound based luminal SRA diameter (mm)	1.27 ± 0.03	1.42 ± 0.04	0.024
Ex vivo morphometry based external SRA diameter (mm)	2.32 ± 0.14	3.14 ± 0.24	0.006
Body weight (gm)	29.08 ± 0.47	28.54 ± 0.47	NS
SBP (mmHg)	130.40 ± 1.75	121.20 ± 1.57	0.029

Data expressed as mean ± S.E.M. for normally distributed data and compared by *t* test or as median and IQRs for non-normally distributed data and compared by Mann–Whitney U test. Statistical significance considered as *P*-value <0.05. Abbreviations: *n*, number; NS, non-significant.

TSP-1 deficiency promoted AngII-induced AAA and atherosclerosis in a mouse model

To further assess the role of TSP-1 in AAA progression, we used the well-established AngII model of AAA [54]. AngII was infused in 12-weeks-old male control *ApoE*$^{-/-}$ (*n*=20) and experimental *Thbs1* and ApoE double-deficient (*Thbs1*$^{-/-}$*ApoE*$^{-/-}$; *n*=20) mice using established protocols. Infusion of AngII for 28 days resulted in aortic ruptures in both *ApoE*$^{-/-}$ (deaths =7; 35%) and *Thbs1*$^{-/-}$*ApoE*$^{-/-}$ mice (deaths =4; 20%), with no significant difference in the rupture rate between the two genotypes (*P*=0.325*;* Supplementary Figures S1–S3). Aortic diameter was assessed *in vivo* using ultrasound to assess the inner wall to the inner wall aortic luminal diameter using sagittal images in the anterior-posterior plane. AngII infusion for 4 weeks caused a progressive increase in the SRA diameter as assessed by ultrasound in *ApoE*$^{-/-}$ and *Thbs1*$^{-/-}$*ApoE*$^{-/-}$ mice. The mean maximum (± S.E.M.) SRA diameter measured by ultrasound on day 28 of the AngII infusion was 1.27 ± 0.03 and 1.42 ± 0.04 mm in the *ApoE*$^{-/-}$ control (*n*=13) and *Thbs1*$^{-/-}$*ApoE*$^{-/-}$ experimental (*n*=16) mice respectively (*P*=0.024, Figure 2A, Table 2). These findings were supported by *ex vivo* morphometric measurements which showed a similar significantly greater mean maximum (± S.E.M.) SRA external (outer wall to outer wall) diameter in *Thbs1*$^{-/-}$*ApoE*$^{-/-}$ (3.14 ± 0.24 mm) compared with *ApoE*$^{-/-}$ (2.32 ± 0.14 mm, *P*=0.006; Figure 2B) mice. Maximum diameters of other aortic regions were similar between groups (Figure 2B).

En face atherosclerosis assessment was performed by Sudan IV staining of aortic arches. The median (IQR) staining area was significantly greater in experimental *Thbs1*$^{-/-}$*ApoE*$^{-/-}$ (23.18%, 20.90–38.28) compared with control *ApoE*$^{-/-}$ (14.06%, 7.48–33.20, *P*=0.049; *n*=8/group; Figure 2D,E) mice.

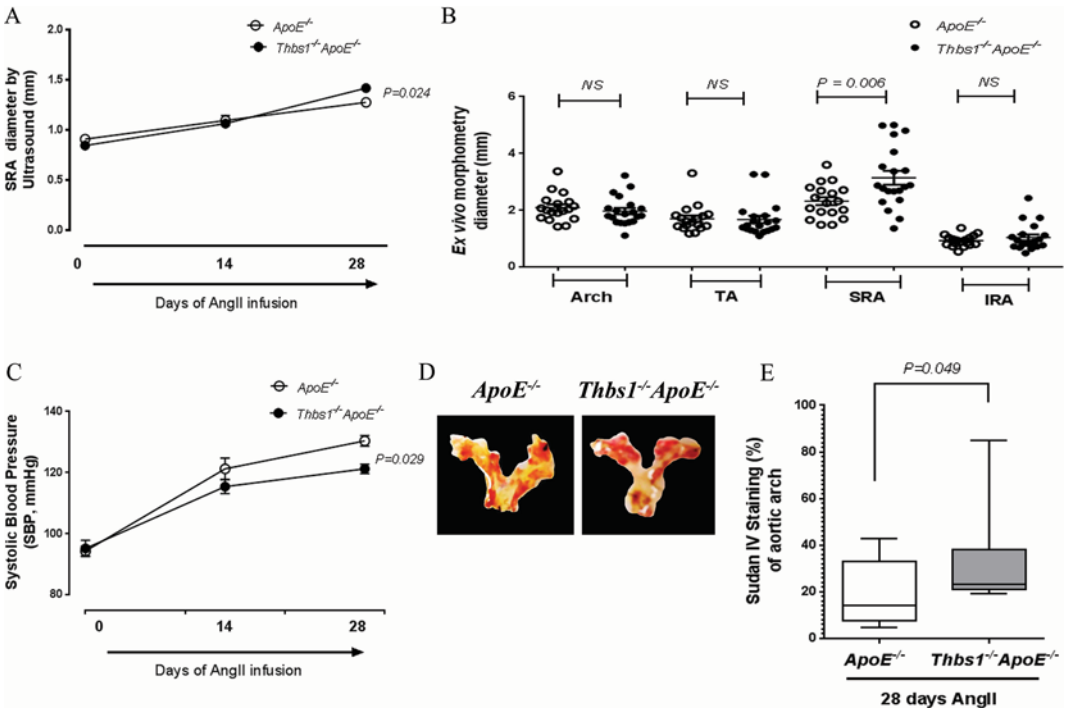

Figure 2. TSP-1 deficiency promotes AAA and atherosclerosis in AngII-infused mice

(**A**) Mean SRA diameter assessed by ultrasound in $ApoE^{-/-}$ (n=13) and $Thbs1^{-/-}ApoE^{-/-}$ (n=16) mice surviving AngII infusion. Data expressed as mean and S.E.M. and compared by repeated measures two-way ANOVA. (**B**) Regional maximum diameters of control $ApoE^{-/-}$ and experimental $Thbs1^{-/-}ApoE^{-/-}$ mice were determined by *ex vivo* morphometric measurements at the end of 28 days of AngII infusion. AngII-infused $Thbs1^{-/-}ApoE^{-/-}$ mice had a significantly larger SRA diameter compared with AngII-infused $ApoE^{-/-}$ mice. Data expressed as median and IQR with maximum and minimum data points (whiskers) and compared by Mann–Whitney U test. (**C**) Graphs comparing the effect of AngII infusion on mean SBP in $ApoE^{-/-}$ and $Thbs1^{-/-}ApoE^{-/-}$ mice. Data expressed as mean and S.E.M. and compared by repeated measures two-way ANOVA. (**D**) Representative *en face* Sudan IV stained aortic arches from control $ApoE^{-/-}$ and experimental $Thbs1^{-/-}ApoE^{-/-}$ mice for quantifying atherosclerosis. (**E**) Box plots showing that aortic arch Sudan IV staining area was significantly higher in experimental $Thbs1^{-/-}ApoE^{-/-}$ than control $ApoE^{-/-}$ mice after 28 days of AngII infusion. Data expressed as median and IQR with maximum and minimum data points (whiskers) for positive staining area relative to total specimen area (%) and compared by Mann–Whitney U test (n=8/group). Abbreviation: NS, non-significant.

$Thbs1^{-/-}ApoE^{-/-}$ mice had lower blood pressure during AngII infusion associated with higher circulating concentrations of nitric oxide metabolites

We compared the systolic blood pressure (SBP) in AngII-infused control $ApoE^{-/-}$ and experimental $Thbs1^{-/-}ApoE^{-/-}$ mice. Chronic infusion of AngII for 28 days caused a significant time-dependent increase in mean SBP in both $ApoE^{-/-}$ and $Thbs1^{-/-}ApoE^{-/-}$ mice (Figure 2C). The mean SBP of the experimental $Thbs1^{-/-}ApoE^{-/-}$ mice and control $ApoE^{-/-}$ mice were similar at baseline, however during the AngII infusion, the SBP was significantly greater in $ApoE^{-/-}$ compared with $Thbs1^{-/-}ApoE^{-/-}$ mice as analysed by repeated measures two-way ANOVA (P=0.029, Figure 2C). Heart rate was similar in both groups throughout the study (results not shown).

Evaluation of total nitrite and nitrate (nitric oxide metabolites) within plasma collected after 28 days of AngII infusion showed significantly higher median levels in experimental $Thbs1^{-/-}ApoE^{-/-}$ (59.87 μM, IQR: 32.79–70.95) compared with the control $ApoE^{-/-}$ mice (27.67 μM, IQR: 4.28–36.04, P=0.041; Table 3).

Clinical Science (2017) **131** 1261–1281
DOI: 10.1042/CS20160970

Table 3 The concentrations of cytokines within the platelet-poor plasma of control *ApoE*$^{-/-}$ and experimental *Thbs1*$^{-/-}$*ApoE*$^{-/-}$ mice infused with AngII for 28 days

Samples	*ApoE*$^{-/-}$ (*n*=8)	*Thbs1*$^{-/-}$*ApoE*$^{-/-}$ (*n*=8)	*P*-value
MCP-1 (pg/ml)	8.52 (6.22–18.61)	47.56 (11.26–77.43)	0.026
IL-6 (pg/ml)	38.86 (17.31–76.94)	250 (44.30–372.80)	0.041
IL-10 (pg/ml)	65.61 (43.83–230.70)	225.30 (58.50–408.10)	0.227
IFN-γ (pg/ml)	74.16 (55.08–200.50)	184.50 (71.01–275.10)	0.278
TNF (pg/ml)	252.50 (42.01–394)	560.30 (346.60–658)	0.063
IL-12p70 (pg/ml)	43.76 (7.28–68.72)	88.77 (19.11–193.50)	0.228
NOx metabolites (nM)	27.67 (4.28–36.04)	59.87 (32.79–70.95)	0.041
Total TGF-β1 (ng/ml)	3.61 ± 0.21	3.74 ± 0.90	0.589
Active TGF-β1 (ng/ml)	0.50 ± 0.04	0.16 ± 0.02	0.001

Concentrations of cytokines (pg/ml) were measured in the platelet-poor plasma (*n*=8/group) using an inflammatory bead assay. NOx metabolites were assessed by Griess assay. Total and active TGF-β1 were assessed by an activity assay. Data expressed as median and IQRs are compared by Mann–Whitney U test. Tgf-β1 data presented as mean ± S.E.M. and analysed by Student's *t* test. Statistical significance considered as *P*-value <0.05. Abbreviations: mTgf, mouse transforming growth factor; NOx, total nitrite and nitrate metabolites.

AngII induced AAA was associated with increased ECM degradation in Thbs1$^{-/-}$ApoE$^{-/-}$ mice

Serial sections of SRA segments were used for morphological assessments by histology. Compared with control *ApoE*$^{-/-}$ mice, experimental *Thbs1*$^{-/-}$*ApoE*$^{-/-}$ mice had increased aortic medial thickness, increased inflammatory cell infiltration, more necrotic regions and bigger intramural thrombus (Figure 3A). The presence of red blood cells and large intramural haematomas was evident in the H&E-stained SRA sections of *Thbs1*$^{-/-}$*ApoE*$^{-/-}$ mice.

EVG staining demonstrated disruption of elastin filaments in both control *ApoE*$^{-/-}$ and *Thbs1*$^{-/-}$*ApoE*$^{-/-}$ (Figure 3B) mice. Quantification of elastin breaks in *ApoE*$^{-/-}$ and *Thbs1*$^{-/-}$*ApoE*$^{-/-}$ SRA sections suggested more severe medial layer disruption in experimental mice. The mean grade (± S.E.M.) of elastin degradation was significantly higher in *Thbs1*$^{-/-}$*ApoE*$^{-/-}$ (3.80 ± 0.12) compared with control *ApoE*$^{-/-}$ mice (2.50 ± 0.46, P= 0.025; n=8/group; Figure 3E).

Increased numbers of apoptotic cells were observed in sections taken from the SRA of experimental *Thbs1*$^{-/-}$*ApoE*$^{-/-}$ compared with control *ApoE*$^{-/-}$ mice (n=6/group) after they had received AngII infusion for 28 days (Figure 3C). TUNEL-positive staining was identified within the intima, adventitia and particularly within the medial elastic lamellae of the SRA in both the groups. TUNEL-positive staining area was significantly greater within the SRA of experimental *Thbs1*$^{-/-}$*ApoE*$^{-/-}$ (median TUNEL staining area: 21.50%, IQR: 19.16–23.05) compared with control *ApoE*$^{-/-}$ mice (median TUNEL staining area: 11.50%, IQR: 8.61–13.41, P=0.002; Figure 3F).

TSP-1 deficiency enhanced the systemic and aortic inflammatory response to AngII infusion

Systemic inflammation was assessed in platelet-poor plasma collected after 28 days of AngII infusion by a multiplexed flow cytometric assay. *Thbs1*$^{-/-}$*ApoE*$^{-/-}$ mice had higher median plasma concentrations of monocyte chemoattractant protein (MCP)-1 (47.56 pg/ml, IQR: 11.26–77.43 compared with 8.52 pg/ml, IQR: 6.22–18.61; P=0.026) and IL-6 (250 pg/ml, IQR: 44.30–372.80 compared with 38.86 pg/ml, IQR: 17.31–76.94; P=0.041) compared with control *ApoE*$^{-/-}$ mice. A similar but non-significant trend was observed for plasma concentrations of IL-10, IL-12p70, IFN-γ and TNF-α (Table 3).

Macrophage infiltration as identified by CD68 staining was observed in sections taken from the SRA of both experimental *Thbs1*$^{-/-}$*ApoE*$^{-/-}$ and control *ApoE*$^{-/-}$ mice (n=6/group) after they had received AngII infusion for 28 days (Figure 3D). Marked CD68 staining was identified within the adventitia and particularly within the tunica media of the SRA in *Thbs1*$^{-/-}$*ApoE*$^{-/-}$ mice (Figure 3D). The median CD68-positive staining area was significantly greater within the SRA of experimental *Thbs1*$^{-/-}$*ApoE*$^{-/-}$ (29.27%, IQR: 22.50–37.50) compared with control *ApoE*$^{-/-}$ mice (20.80%, IQR: 15.01–24.81, P=0.041; Figure 3G).

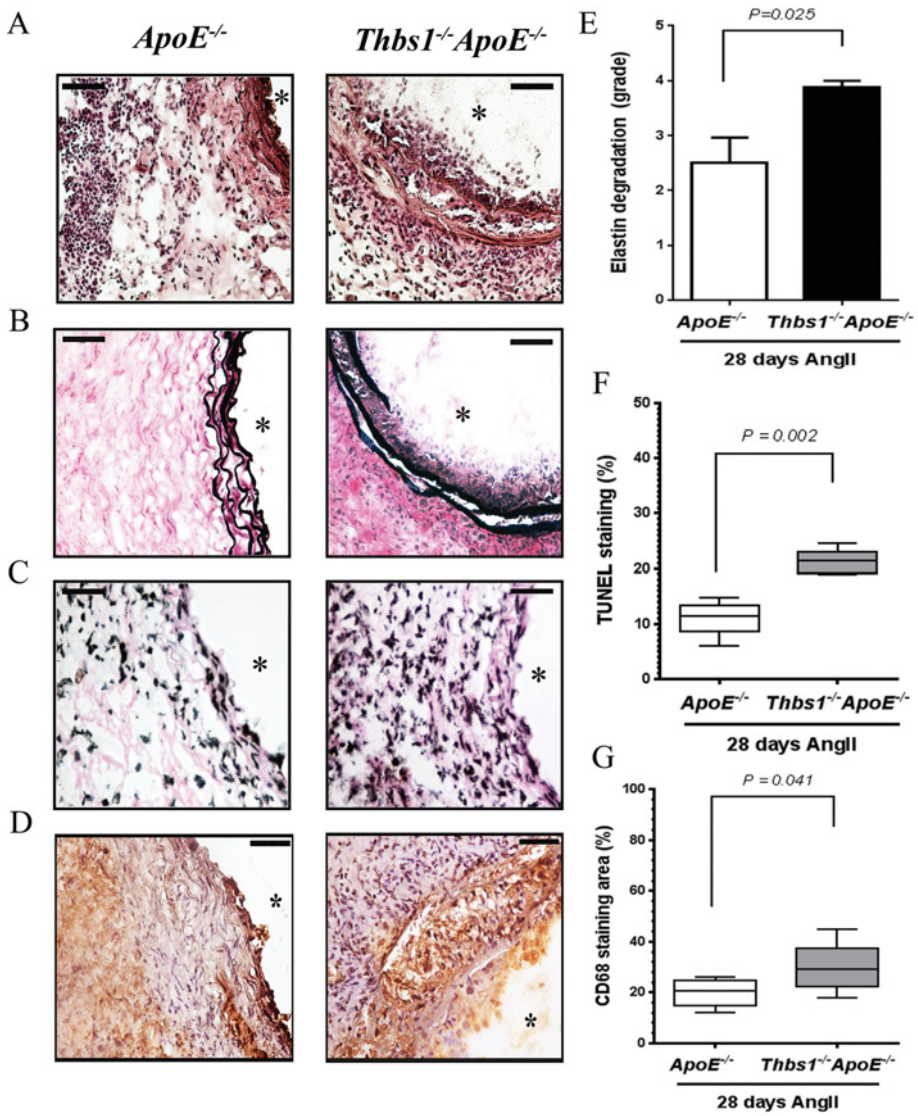

Figure 3. Histological features of AngII infused AAA in *Thbs1*$^{-/-}$*ApoE*$^{-/-}$ mice

(**A**) Representative light microscope images of H&E staining showing medial and intimal inflammatory cell infiltration in *ApoE*$^{-/-}$ and *Thbs1*$^{-/-}$*ApoE*$^{-/-}$ mice infused with AngII for 28 days. Increased medial thickening and intramural inflammatory cell infiltration was noted in the SRA of *Thbs1*$^{-/-}$*ApoE*$^{-/-}$ mice. Original magnification ×400. Scale bars =50 μm. (**B**) Representative EVG staining (black after staining with EVG) showing greater focal elastin breaks along with marked neointima formation in *Thbs1*$^{-/-}$*ApoE*$^{-/-}$ mice compared with the control *ApoE*$^{-/-}$. Scale bars =50 μm. (**C**) Representative photomicrograph showing that TSP-1 deficiency promotes apoptosis. Detection of apoptosis was performed by TUNEL assay using the VasoTACS *in situ* apoptosis detection kit in SRA sections of *ApoE*$^{-/-}$ and *Thbs1*$^{-/-}$*ApoE*$^{-/-}$ mice infused with AngII for 28 days. Representative TUNEL staining showing increased presence of apoptotic and disintegrated cells in *Thbs1*$^{-/-}$*ApoE*$^{-/-}$ mice infused with AngII. Original magnification ×400. Scale bars =50 μm. (**D**) Representative microscopy images of macrophage staining using rat anti-mouse CD68 antibody in AngII-infused *ApoE*$^{-/-}$ and *Thbs1*$^{-/-}$*ApoE*$^{-/-}$ mice. (**E**) Quantification of elastin breaks in *ApoE*$^{-/-}$ and *Thbs1*$^{-/-}$*ApoE*$^{-/-}$ mice within SRA sections. Elastin breaks were quantified based on previously published criteria (see 'Materials and methods' section). The numbers of elastin breaks were higher in *Thbs1*$^{-/-}$*ApoE*$^{-/-}$ compared with control *ApoE*$^{-/-}$ mice. Results are mean ± S.E.M. elastin degradation grade. Statistical analysis by Fisher's exact tests for *n*=8/group. (**F**) Quantification graph of TUNEL staining in SRA sections of *ApoE*$^{-/-}$ and *Thbs1*$^{-/-}$*ApoE*$^{-/-}$ mice. Shown is data expressed as median and IQR with maximum and minimum data points (whiskers) for positive staining area relative to total specimen area (%) and compared by Mann–Whitney U test (*n*=6/group). (**G**) Quantificative analysis of macrophage infiltration within the SRA specimens was performed by evaluating the area of CD68-positive staining in non-necrotic areas. The results are presented as a percentage of CD68-positive staining area in sections from AngII infused *ApoE*$^{-/-}$ compared with *Thbs1*$^{-/-}$*ApoE*$^{-/-}$ mice. Data expressed as median and IQR with maximum and minimum data points (whiskers) and compared by Mann–Whitney U test (*n*=6/group).

Clinical Science (2017) **131** 1261–1281
DOI: 10.1042/CS20160970

Table 4 Relative expression of genes within the SRA of control *ApoE*$^{-/-}$ and experimental *Thbs1*$^{-/-}$*ApoE*$^{-/-}$ mice infused with AngII for 28 days

Genes	Sample	Genotype	Median expression (IQR)	*P*-value
Mmp-9	*SRA* (*n*=6)	*ApoE*$^{-/-}$	0.29 (0.11–0.63)	0.026
		Thbs1$^{-/-}$*ApoE*$^{-/-}$	0.97 (0.70–1.27)	
Col1A1	*SRA* (*n*=6)	*ApoE*$^{-/-}$	1.95 (1.56–4.37)	0.041
		Thbs1$^{-/-}$*ApoE*$^{-/-}$	1.47 (1.14–1.77)	
	VSMC (*n*=6)	*ApoE*$^{-/-}$	0.70 (0.20–3.08)	0.787
		Thbs1$^{-/-}$*ApoE*$^{-/-}$	0.51 (0.32–0.72)	
Col3A1	*SRA* (*n*=6)	*ApoE*$^{-/-}$	2.21 (1.35–6.50)	0.015
		Thbs1$^{-/-}$*ApoE*$^{-/-}$	0.30 (0.04–1.45)	
	VSMC (*n*=6)	*ApoE*$^{-/-}$	2.78 (1.15–3.76)	0.015
		Thbs1$^{-/-}$*ApoE*$^{-/-}$	0.17 (0.10–1.25)	
Lrp1	*SRA* (*n*=6)	*ApoE*$^{-/-}$	2.66 (1.99–5.13)	0.015
		Thbs1$^{-/-}$*ApoE*$^{-/-}$	1.02 (0.55–1.74)	
	VSMC (*n*=6)	*ApoE*$^{-/-}$	1.03 (0.32–1.92)	0.041
		Thbs1$^{-/-}$*ApoE*$^{-/-}$	0.25 (0.17–0.47)	

Data expressed as median and IQRs and compared by Mann–Whitney U test. Statistical significance considered as *P*-value <0.05. Abbreviations: LRP, low-density receptor related protein; *n*, number of mice.

Plasma concentrations of active TGF-β1 were lower in Thbs1$^{-/-}$ApoE$^{-/-}$ mice than control mice but markers of TGF-β1 signalling were not different in aortic samples from Thbs1$^{-/-}$ApoE$^{-/-}$ and control mice

The levels of total and active TGF-β1 were assessed within the platelet-poor plasma from mice collected after 28 days of AngII infusion. Plasma concentrations of total TGF-β1 were similar in *ApoE*$^{-/-}$ and *Thbs1*$^{-/-}$*ApoE*$^{-/-}$ mice. Plasma levels of active TGF-β1 were significantly lower in *Thbs1*$^{-/-}$*ApoE*$^{-/-}$ compared with *ApoE*$^{-/-}$ mice (0.16 ± 0.02 ng/ml compared with 0.50 ± 0.04 ng/ml, *P*=0.001; Table 3). Analysis of SRA lysates by Western blotting demonstrated that levels of aortic tissue p-*Smad2/3* to total-*Smad2/3* were not significantly different in the *Thbs1*$^{-/-}$*ApoE*$^{-/-}$ mice compared with *ApoE*$^{-/-}$ mice (Supplementary Figure S4). In addition, the level of aortic tissue p-*Akt* to total-*Akt* was also not significantly different in *Thbs1*$^{-/-}$*ApoE*$^{-/-}$ mice compared with *ApoE*$^{-/-}$ mice (Supplementary Figure S5).

TSP-1 deficiency enhanced systemic and aortic MMP-9 expression

Prior to AngII infusion, the level of plasma MMP-9 was significantly higher in *Thbs1*$^{-/-}$*ApoE*$^{-/-}$ (162.50 ± 14.05 ng/ml) compared with *ApoE*$^{-/-}$ (75.06 ± 9.32 ng/ml, *P*<0.001) mice. AngII infusion for 28 days resulted in increased MMP-9 concentrations in the plasma of both the groups with higher mean (± S.E.M.) levels of MMP-9 in *Thbs1*$^{-/-}$*ApoE*$^{-/-}$ compared with the *ApoE*$^{-/-}$ (210.50 ± 27.05 ng/ml compared with 121 ± 25.20 ng/ml, *P*=0.030) mice. Quantitative real-time PCR analysis of mRNA extracted from the SRA of mice infused with AngII for 28 days showed significantly higher relative expression of *Mmp-9* in *Thbs1*$^{-/-}$*ApoE*$^{-/-}$ (median relative gene expression: 0.97, IQR: 0.70–1.27) compared with control *ApoE*$^{-/-}$ mice (median relative gene expression: 0.29, IQR: 0.11–0.63, *P*=0.026, Table 4).

We also assessed gelatinase activity within SRA sections from mice infused with AngII for 28 days using *in situ* zymography. The gelatinase activity was marked within the media and adventitia of *Thbs1*$^{-/-}$*ApoE*$^{-/-}$ compared with control *ApoE*$^{-/-}$ mice (Figure 4A). A semiquantitative analysis of gelatinase activity (% positivity relative to the whole-section area) was performed in cryostat sections of SRA segments. The median gelatinase activities were 30.50% (IQR: 26.34–40.82) and 21.04% (IQR: 15.12–28.07, *P*=0.041; *n*=6/group) in experimental *Thbs1*$^{-/-}$*ApoE*$^{-/-}$ and control *ApoE*$^{-/-}$ mice respectively (Figure 4B).

TSP-1 deficiency was associated with decreased collagen content and reduced LRP1 expression within the SRA

The collagen content of SRA sections was analysed by Picrosirius Red staining followed by polarization microscopy and image analysis. There was significantly less fibrillar collagen within SRA sections taken from *Thbs1*$^{-/-}$*ApoE*$^{-/-}$

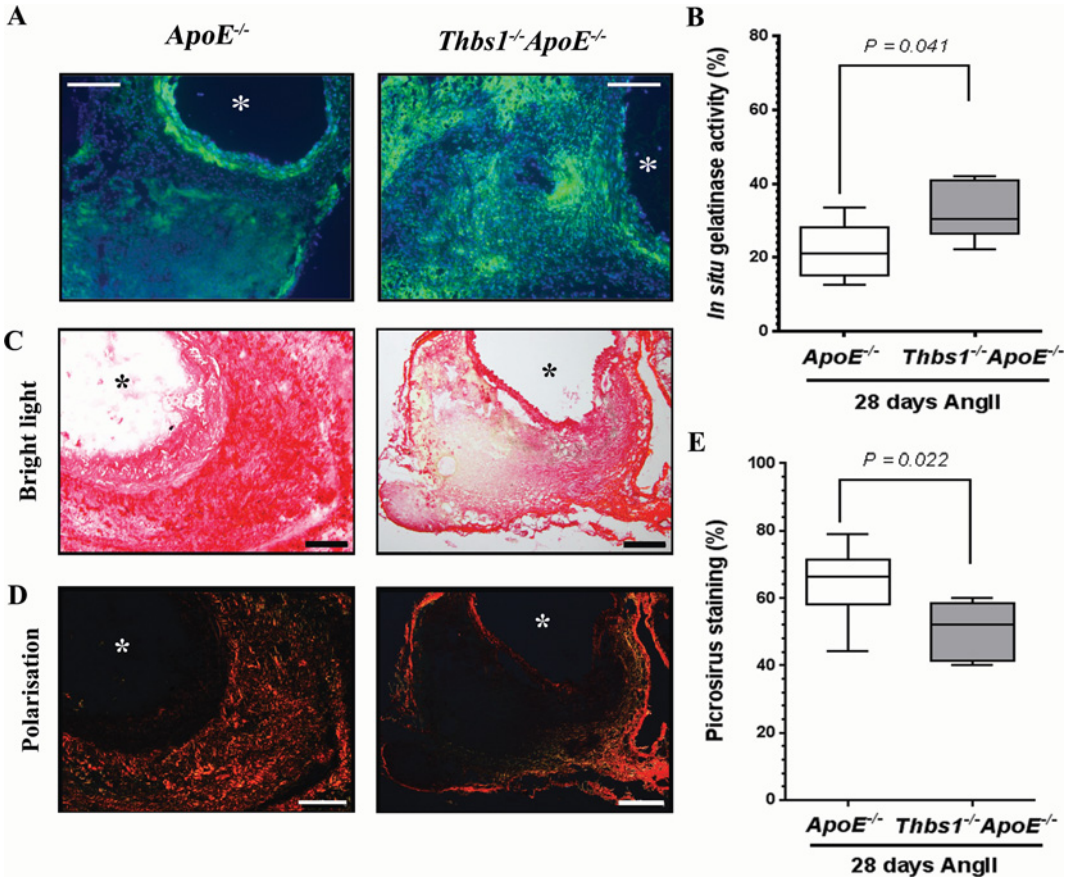

Figure 4. TSP-1 deficiency aggravates inflammation and promotes matrix degradation in AngII-infused AAA

(**A**) Representative photomicrograph of *in situ zymography* showing that absence of TSP-1 induces increased MMP-gelatinase activity within the SRA. MMP-gelatinase activity is evident as green fluorescence signal and elastin lamellae are stained blue under fluorescent microscopy. Original magnification ×400. Scale bars =50 μm. The $Thbs1^{-/-}ApoE^{-/-}$ SRA showed marked elevation in the gelatinolytic area. (**B**) Semiquantitative analysis (% positivity relative to the whole section) of MMP-gelatinase activity in SRA sections of control $ApoE^{-/-}$ and experimental $Thbs1^{-/-}ApoE^{-/-}$ mice infused with AngII for 28 days. Elastin lamellae are stained blue. Data expressed as median and IQR with maximum and minimum data points (whiskers) and compared by Mann–Whitney U test (n=6/group). (**C**) Representative bright-field images of Picrosirius staining in AngII-infused $ApoE^{-/-}$ and $Thbs1^{-/-}ApoE^{-/-}$ mice. (**D**) Representative polarization microscopy images of Picrosirius staining in AngII-infused $ApoE^{-/-}$ and $Thbs1^{-/-}ApoE^{-/-}$ mice. Quantitative analysis of collagen deposition in the SRA specimens was performed by evaluating the polarization birefringence image staining. (**E**) Quantitative analysis of collagen staining in the SRA sections was performed by evaluating the percentage of birefringent staining area in the AngII infused $ApoE^{-/-}$ compared with $Thbs1^{-/-}ApoE^{-/-}$ mice under polarized light. Data expressed as median and IQR with maximum and minimum data points (whiskers) and compared by Mann–Whitney U test (n=6/group). For all images, original magnification ×400. Scale bars =50 μm. * denotes lumen.

compared with $ApoE^{-/-}$ mice (Figure 4C, D). The collagen content was not evenly distributed but localized in deposits in the dilated aneurysmal regions with clear necrotic areas in between suggesting reduced synthesis of new collagen deposits. Under polarization imaging, the SRA sections of $Thbs1^{-/-}ApoE^{-/-}$ mice showed less collagen birefringence compared with the SRA sections of $ApoE^{-/-}$ mice ($Thbs1^{-/-}ApoE^{-/-}$ median % birefringence area: 52.24%, IQR: 41.36–58.34 compared with $ApoE^{-/-}$ 66.49%; IQR: 58.12–71.45, n=6/group; P=0.022; Figure 4E). We also assessed the transcript levels of two major collagen genes in mRNA isolated from SRA segments by qRT-PCR. The median relative *Col1A1* mRNA expression was lower in $Thbs1^{-/-}ApoE^{-/-}$ compared with $ApoE^{-/-}$ mice (median relative gene expression: 1.47, IQR: 1.14–1.77 compared with 1.95, IQR: 1.56–4.37, P=0.041, Table 4). Similarly, the median relative *Col3A1* mRNA expression was significantly lower in $Thbs1^{-/-}ApoE^{-/-}$ compared with $ApoE^{-/-}$ mice (median relative gene expression: 0.30, IQR: 0.04–1.45 compared with 2.21, IQR: 1.35–6.50, P=0.015; Table 4).

Since VSMCs are the predominant source of collagen in arteries and to assess the expression of collagen genes in the early phases of matrix remodelling, we infused $ApoE^{-/-}$ and $Thbs1^{-/-}ApoE^{-/-}$ mice (n=6/group) with AngII

Clinical Science (2017) **131** 1261–1281
DOI: 10.1042/CS20160970

for 14 days and then isolated VSMCs from the SRA segments. The median relative expression of *Col1A1* was similar in the two groups of mice (Table 4). *Col3A1* expression was lower in VSMCs isolated from $Thbs1^{-/-}ApoE^{-/-}$ mice (median relative gene expression: 0.17, IQR: 0.10–1.25 compared with 2.78, IQR: 1.15–3.76, P=0.015) supporting the altered phenotype of VSMCs in the SRA of $Thbs1^{-/-}ApoE^{-/-}$ mice (Table 4).

TSP-1 binds to LRP1 to signal changes in cell adhesion and motility [55,56]. LRP1 has also been implicated in maintaining normal aortic structure since deficiency is associated with spontaneous aneurysm formation in mice [57]. We infused 3-month-old male $ApoE^{-/-}$ mice with saline (n=3) and AngII (n=3) for 28 days to assess the effect of AngII on expression of LRP1. Confocal microscopy suggested that the expression of LRP1 protein within the SRA was up-regulated after 28-day infusion of AngII (Figure 5A). LRP1 protein expression was mainly localized within the media with diffuse expression throughout the adventitia. Given the link between LRP1 and TSP-1, we examined the relative gene expression of *Lrp1* in SRA segments obtained from $Thbs1^{-/-}ApoE^{-/-}$ and $ApoE^{-/-}$ mice after 28 days AngII infusion. The relative expression of *Lrp1* was significantly lower in $Thbs1^{-/-}ApoE^{-/-}$ (median relative gene expression: 1.02, IQR: 0.55–1.74) compared with $ApoE^{-/-}$ mice (median relative gene expression: 2.66, IQR 1.99–5.13, P=0.015, Table 4, Figure 5B). We also compared the expression of *Lrp1* transcripts in VSMCs isolated from SRA segments of mice infused with AngII for 14 days. The relative expression of *Lrp1* was significantly lower in VSMCs isolated from $Thbs1^{-/-}ApoE^{-/-}$ (median relative gene expression: 0.25, IQR: 0.17–0.47) compared with $ApoE^{-/-}$ mice (median relative gene expression: 1.03, IQR: 0.32–1.92, P=0.041, Figure 5C).

Discussion

The main findings of the present study were that higher circulating concentrations of TSP-1 were associated with slower AAA growth in patients, and that within a mouse model, TSP-1 deficiency promoted larger AAAs. AAA patients with serum concentrations in the highest quartile were less likely to have AAA growth greater than median. This observation is in accordance with our previous report that serum TSP-1 was negatively associated with AAA diagnosis in men after adjusting for other risk factors [23]. This previous proteomic analysis of intraluminal thrombus conducted in our laboratory identified a group of proteins, including TSP-1, to be concentrated in AAA thrombus suggesting this may lead to lower circulating levels of these proteins [23]. A recent study reported that AAA tissues showed higher TSP-1 expression levels by IHC compared with organ donor aortic wall samples [26]. However, in our current study, IHC results suggested that TSP-1 was sparsely expressed within the main body of the wall of the AAA compared with the higher expression levels in relatively disease-free AAA neck. Given the relative deficiency of TSP-1 within the AAA wall and plasma in patients, we examined the effect of TSP-1 deficiency in a mouse model. We found that deficiency of *Thbs1* in $ApoE^{-/-}$ mice resulted in larger AAAs and increased atherosclerosis in response to AngII infusion.

Deficiency of TSP-1 has been reported to show contrasting effects in different experimental studies [26,28,29,58]. Lack of TSP-1 has been reported to promote inflammatory response to retinal injury and inflammatory mediated lung injury in C57BL/6 mice [28,58]. TSP-1 deficiency has also been reported to promote inflammation within atherosclerotic plaques of $ApoE^{-/-}$ mice [29]. In contrast, TSP-1 deficiency in C57BL/6 mice was reported to limit inflammation and aneurysm formation induced by aortic infusion of elastase or peri-adventitial application of calcium phosphate [26]. Our findings therefore contrast markedly from those of Liu et al. [26] but are consistent with our previous work and the findings of other investigators [24]. Our observations are also in accordance with those by Moura et al. [29], who reported that aortic macrophage infiltration was twice as high in $Thbs1^{-/-}ApoE^{-/-}$ compared with $ApoE^{-/-}$, which coincided with a 30-fold increase in elastin lamina degradation and accumulation of MMP-9. Overall, these findings suggest that in the presence of concurrent atherosclerosis, as found in $ApoE^{-/-}$ mice and AAA patients, deficiency of TSP-1 promotes AAA. In the absence of atherosclerosis, TSP-1 is reported to have pro-aneurysmal effects however given the almost universal presence of atherosclerosis in AAA patients, that situation would be expected to be less relevant to patients. The findings of Liu and colleagues may be more relevant to human thoracic aortic aneurysm in which monogenetic mutations often lead to early presentation of disease in the absence of atherosclerosis [26]. It is interesting to note that we did not find any propensity to thoracic aortic aneurysm in $Thbs1^{-/-}ApoE^{-/-}$ mice subjected to AngII infusion.

Previous studies have suggested that the elevation of blood pressure during AngII infusion is not causal in AAA or atherosclerosis progression induced by AngII [54,59,60]. In the present study, both control $ApoE^{-/-}$ and $Thbs1^{-/-}ApoE^{-/-}$ showed time-dependent increase in SBP during AngII infusion. However, the SBP increase in $Thbs1^{-/-}ApoE^{-/-}$ mice was less severe than that in $ApoE^{-/-}$ mice. Previous studies suggest that TSP-1 is able to modulate blood pressure through increasing nitric oxide production [61]. In the current study, we found elevated nitrate levels in the plasma of AngII-infused $Thbs1^{-/-}ApoE^{-/-}$ mice in comparison with control animals. These

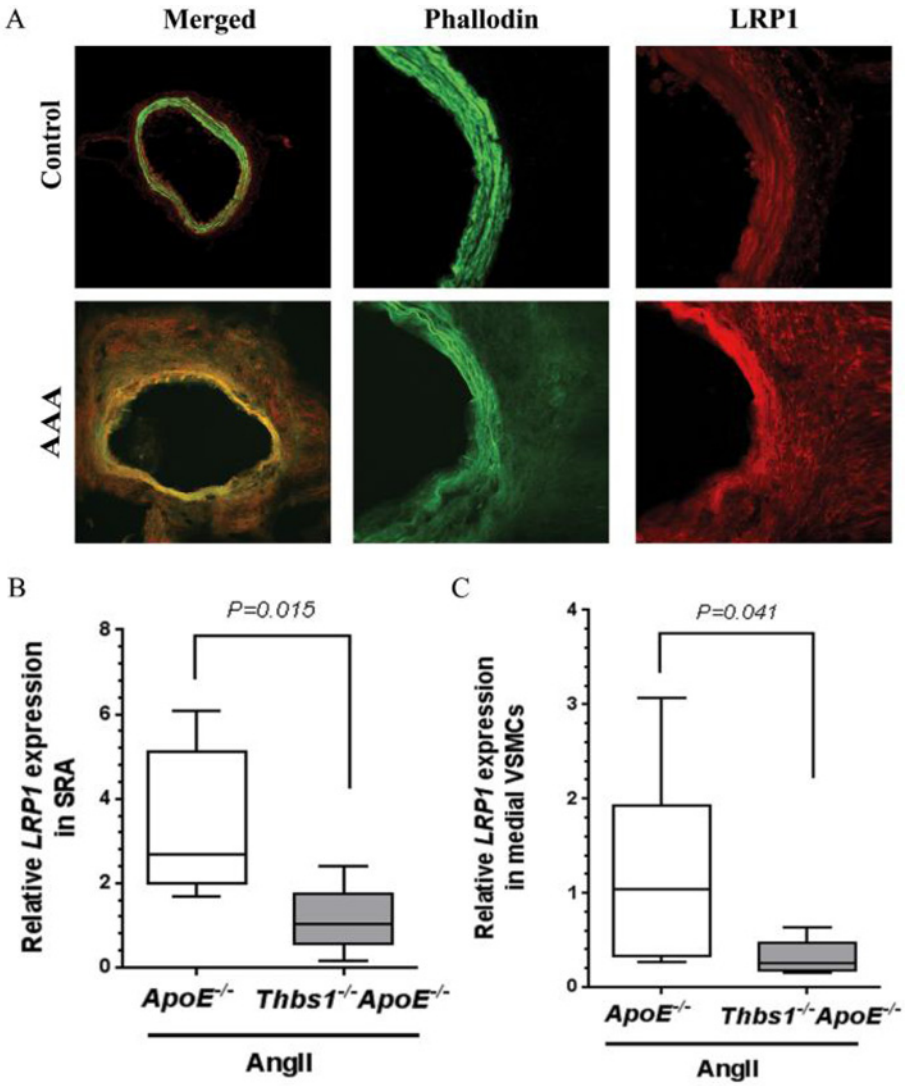

Figure 5. TSP-1 deficiency alters LRP1 expression in AngII-infused AAA

(**A**) Representative confocal images showing typical LRP1 staining in Ang-II infused AAA in *ApoE*$^{-/-}$ mice. The first panel of merged images shows sections of the SRA from saline-infused control *ApoE*$^{-/-}$ and AngII-infused *ApoE*$^{-/-}$ mice. The green staining is phalloidin (actin) and the red staining is LRP1. The confocal images show enhanced LRP1 expression in the SRA of an AngII-infused *ApoE*$^{-/-}$ mouse. The merged images in the first panel is 1417 μm × 1417 μm. The zoomed-in images in the second and third panels are 290 μm × 290 μm. (**B**) Expression of the *Lrp1* within the SRA of AngII-infused *ApoE*$^{-/-}$ and *Thbs1*$^{-/-}$*ApoE*$^{-/-}$ mice. Quantitation graphs depict decreased expression of *Lrp1* within SRA segments of *Thbs1*$^{-/-}$*ApoE*$^{-/-}$ compared with the control *ApoE*$^{-/-}$ mice. Data are expressed as median and IQR with maximum and minimum data points (whiskers) for relative gene expression. Statistical significance calculated with non-parametric Mann–Whitney test (n=8/group). (**C**) Expression of the *Lrp1* within VSMCs from AngII-infused *ApoE*$^{-/-}$ and *Thbs1*$^{-/-}$*ApoE*$^{-/-}$ mice. Quantitation graph depicts decreased expression of *Lrp1* within VSMCs isolated from SRA segments of *Thbs1*$^{-/-}$*ApoE*$^{-/-}$ compared with the control *ApoE*$^{-/-}$ after AngII infusion for 14 days. Data are expressed as median and IQR with maximum and minimum data points (whiskers) for relative gene expression. Statistical significance calculated with non-parametric Mann–Whitney test.

results suggest that the deficiency of TSP-1 results in increased nitric oxide bioavailability and less marked SBP rise in response to AngII infusion. They also agree with previous findings that AAA formation induced by AngII is independent of changes in SBP [54].

Inflammation is implicated in AAA [62,63]. Our results suggest that the absence of TSP-1 promotes systemic and aortic inflammation in response to AngII infusion. This result is in accordance with several previous reports suggesting that TSP-1 inhibits inflammation [29,64–67]. In the current study, active plasma TGF-β1 levels were considerably

Clinical Science (2017) **131** 1261–1281
DOI: 10.1042/CS20160970

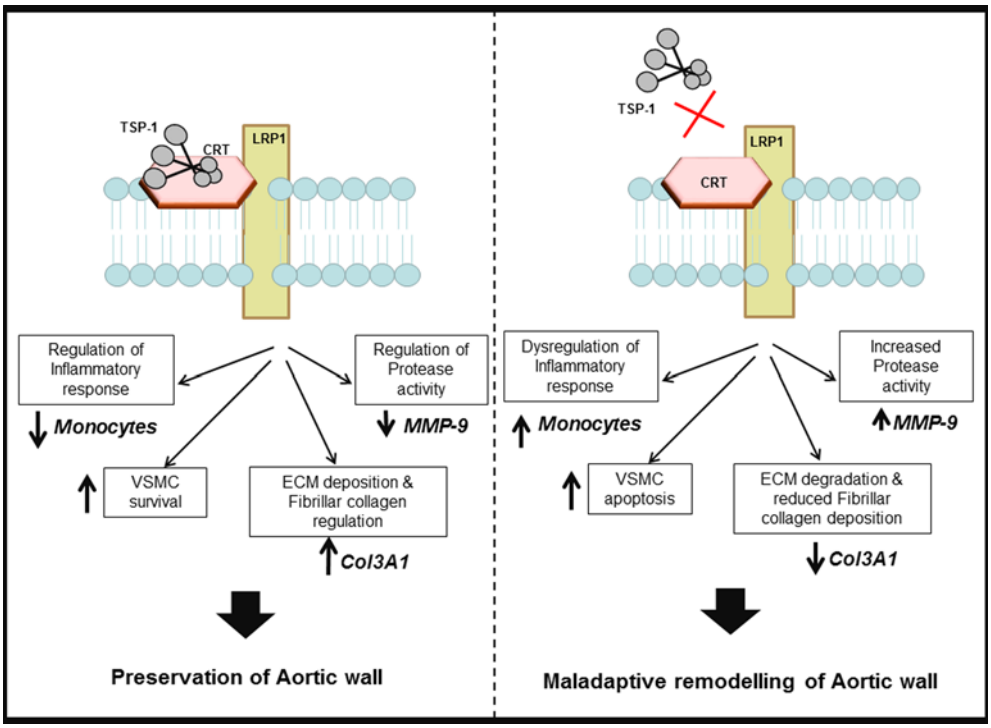

Figure 6. Proposed working model of the protective effect of cell signalling in response to TSP-1 binding to the LRP1 receptor co-complex in the aortic wall

TSP-1 binds to CRT through the N-terminal trimer or the TSP-1 CRT binding peptide (hep I). Binding of TSP-1 to the CRT-LRP1 co-complex leads to the activation of several signalling pathways resulting in: regulation of the inflammatory response, increasing VSMC survival, preservation of elastin, deposition of fibrillar collagen (Col3A1), regulation of proteolytic activity, resulting in the preservation of the aortic wall. However, in the absence of TSP-1, the reduced LRP1 expression leads to aberrant up-regulation of these signalling pathways leading to an increased inflammatory response, especially monocyte infiltration, increased VSMC apoptosis, increased ECM degradation due to degradation of elastin layers and reduced deposition of Col3A1 and increased matrix degradation due to increased MMP-9 levels. The dysregulating of the TSP-1-LRP1 signalling pathway results in maladaptive remodelling leading to development and progression of aortic aneurysm. Abbreviation: CRT, calreticulin.

lower in $Thbs1^{-/-}ApoE^{-/-}$ than control mice. Subsequent analysis of downstream *Smad2/3* and *Akt* phosphorylation suggested however that the TGF-β1 signalling pathway was not activated in $Thbs1^{-/-}ApoE^{-/-}$ mice. Thus, our results suggest that defective TGF-β1 activation is not responsible for the predisposition of $Thbs1^{-/-}ApoE^{-/-}$ mice for AngII-induced AAA and atherosclerosis. Our findings are similar to a previous report that $Thbs1^{-/-}ApoE^{-/-}$ and $ApoE^{-/-}$ mice had similar *Smad2/3* phosphorylation levels [29].

AngII infusion in mice promotes disruption of elastin fibres, enhanced apoptosis and proteolytic destruction of the medial ECM [68,69]. We noted higher elastin degradation and enhanced apoptosis in $Thbs1^{-/-}ApoE^{-/-}$ mice compared with the control $ApoE^{-/-}$ mice. VSMC loss due to apoptosis is believed to be a crucial step in AAA progression [70] and TSP-1 is known to be involved in the clearance of apoptotic neutrophils and eosinophils by macrophages [71,72]. The increased apoptotic cell numbers observed in the SRA of $Thbs1^{-/-}ApoE^{-/-}$ mice could be due to the defective clearance of apoptotic cells rather than an increased apoptosis *per se*.

MMP-9 has been implicated in AAA formation, progression and rupture [73]. In the current study, deficiency of TSP-1 was associated with a marked increase in MMP-9 expression and gelatinase activity within the SRA. The level of plasma MMP-9 was higher in $Thbs1^{-/-}ApoE^{-/-}$ than control mice both prior to and after AngII infusion. This is in accordance with a previous report in a mouse model of dermal wound healing in $Thbs1^{-/-}$ mice in which increased levels of matrix proteolysis enzymes and aberrant ECM remodelling were reported [74,75]. TSP-1 was also reported to attenuate gelatinase activity through its carboxy-terminal fragment [76] by up-regulating tissue inhibitor of MMP (TIMP)-2 (TIMP-2) expression and inhibiting the activity of MMP-9 [77]. Since macrophages are important sources of MMPs, the marked accumulation of macrophages in $Thbs1^{-/-}ApoE^{-/-}$ mice may have promoted the increased

systemic and aortic MMP production [78]. Taken together, our observations are in accordance with previous reports suggesting that enhanced matrix degradation due to elevated MMP-9 occurs in the absence of TSP-1.

The fibrillar collagen network, mainly type III collagen, provides tensile strength to the aortic wall. Previous studies suggest that collagen turnover is ineffective in AAA patients [79–86]. It is postulated that as AAA progresses, the synthesis and structure of collagen is insufficient to counteract increased mechanical wall stress and as a consequence the AAA expands and ruptures [82]. We found reduced *Col3A1* expression in VSMC isolated from $Thbs1^{-/-}ApoE^{-/-}$ mice suggesting that TSP-1 deficiency influenced the response of VSMCs to AngII. This may have played a role in the ability of the aorta to withstand inflammation and proteolysis induced by AngII infusion. Despite this, *Thbs1* deficiency was not associated with increased incidence of AAA rupture, although our study may have not been adequately powered to test this.

LRP1 is a large endocytic receptor that belongs to the LDLR family. A critical role for LRP1 was recently reported to be maintaining the integrity of vessels by regulating protease activity as well as ECM deposition [87]. Reduced LRP1 expression in the aneurysmal wall is reported to be due to the increased shedding of the LRP1 ectodomain as a consequence of heightened inflammation and MMP activity [88]. A genetic polymorphism in LRP has been associated with AAA and within a mouse model deficiency of LRP1 has been associated with aortic aneurysm formation [87,89,90]. Our observation in $ApoE^{-/-}$ mice suggests that AngII infusion leads to LRP1 up-regulation and in the absence of TSP-1, LRP1 expression is down-regulated. Furthermore, our recent study showed that LRP1 expression was lower in AAA patient biopsies compared with controls, and that *in vitro* blockade of LRP1 significantly reduced the ability of VSMCs to clear MMP-9 [91]. These findings suggest that TSP-1 deficiency might promote AAA by the associated down-regulation of LRP1 and Col3A1 and up-regulation of MMP-9 (Figure 6).

The present study has a number of limitations. The clinical findings in the present study are restricted to men and have unknown relation to AAAs in women [92]. Another limitation of the present study is that we used only one mouse model of AAA, although previous studies have been performed in other models which do not typically incorporate atherosclerosis. The results could have also been strengthened by including experiments to investigate if TSP-1 administration corrected the AAA propensity of $Thbs1^{-/-}ApoE^{-/-}$ mice.

In conclusion, the present study suggests AAA growth is promoted by TSP-1 deficiency. Based on our findings and that of other investigators, it seems likely that the effects of TSP-1 are context dependent and our experimental findings may be particularly relevant to aortic aneurysms formed in association with atherosclerosis. Our findings suggest the importance of TSP-1 as a matrix protein protecting the integrity of the aortic ECM.

Clinical perspectives

- The role of TSP-1 in aortic aneurysm is conflicting.
- Circulating TSP-1 levels were negatively correlated with aortic aneurysm growth and men with TSP-1 in the highest quartile had a reduced likelihood of aortic aneurysm growth.
- Knockout of the TSP-1 gene in $ApoE^{-/-}$ mice and induction of aortic aneurysm using AngII infusion generated larger aneurysms, which were also associated with greater inflammation, increased apoptosis and increased ECM degradation.
- These clinical and preclinical observations are novel and suggest potential important implications for treating AAA.

Acknowledgements

We thank Prof William A. Frazier, Washington University School of Medicine, U.S.A. for supplying the $Thbs1^{-/-}$ mice used for breeding in the present study.

Funding

This work was supported by the National Health and Medical Research Council [grant numbers 1000967, 540404, 1021416, 1079193, 1079369, 1098717]; the Office of Health and Medical Research; the Practitioner Fellowship from the National Health and Medical Research Council, Australia [grant number 1117061 (to J.G.)]; and the Senior Clinical Research Fellowship from the Queensland Government.

Clinical Science (2017) **131** 1261–1281
DOI: 10.1042/CS20160970

Author contribution

S.M.K. designed and performed the mouse work and *in vitro* studies, analysed the data, and drafted the manuscript; S.M.K. and J.L. performed histology and IHC; S.W.S. and R.J.J. performed FACS analysis and molecular work; J.M. and P.C. performed ELISA assays. T.I.E. assisted with the animal model and ultrasound analysis; D.J.C. performed the confocal analysis; P.N. provided patient samples and clinical data; J.G. prepared applications for and obtained funding and contributed to the experimental design, data analysis and interpretation, and edited the paper prior to submission. All authors contributed to critical revision of the manuscript and approved the final version of the manuscript to be published.

Competing interests

The authors declare that there are no competing interests associated with the manuscript.

Abbreviations

AAA, abdominal aortic aneurysm; AngII, angiotensin II; ApoE, apolipoprotein E; *ApoE*$^{-/-}$, apolipoprotein E deficient; CBA, cytometric bead array; CHD, coronary heart disease; CI, confidence interval; *Col1A1*, collagen type 1A1; *Col3A1*, collagen type 3A1; CRP, C-reactive protein; ECM, extracellular matrix; EVG, Elastin Van Gieson; GAPDH, glyceraldehyde-3-phosphate dehydrogenase; HDL, high-density lipoprotein; HIMS, Health In Men Study; H&E, haematoxylin and eosin; IFN, interferon; IHC, immunohistochemistry; IL, interleukin; IQR, interquartile range; LDL, low-density lipoprotein; LRP1, low-density lipoprotein receptor-related protein 1; MCP-1, monocyte chemoattractant protein-1; MMP, matrix metalloproteinase; qRT-PCR, quantitative real-time PCR; SBP, systolic blood pressure; SRA, suprarenal aorta; TA, thoracic aorta; Tgf-β, transforming growth factor β; *Thbs1*$^{-/-}$, thrombospondin-1 deficient; TNF, tumour necrosis factor; TSP-1, thrombospondin-1; TUNEL, terminal deoxynucleotidyl transferase mediated dUTP nick-end labelling; VSMC, vascular smooth muscle cell.

References

1 Golledge, J., Muller, J., Daugherty, A. and Norman, P. (2006) Abdominal aortic aneurysm: pathogenesis and implications for management. *Arterioscler. Thromb. Vasc. Biol.* **26**, 2605–2613
2 Golledge, J. and Norman, P.E. (2009) Pathophysiology of abdominal aortic aneurysm relevant to improvements in patients' management. *Curr. Opin. Cardiol.* **24**, 532–538
3 Wanhainen, A., Hultgren, R., Linne, A., Holst, J., Gottsater, A., Langenskiold, M. et al. (2016) Outcome of the Swedish Nationwide Abdominal Aortic Aneurysm Screening Program. *Circulation* **134**, 1141–1148
4 Jones, G.T., Hill, B.G., Curtis, N., Kabir, T.D., Wong, L.E., Tilyard, M.W. et al. (2016) Comparison of three targeted approaches to screening for abdominal aortic aneurysm based on cardiovascular risk. *Br. J. Surg.* **103**, 1139–1146
5 United Kingdom Small Aneurysm Trial Participants (2002) Long-term outcomes of immediate repair compared with surveillance of small abdominal aortic aneurysms. *N. Engl. J. Med.* **346**, 1445–1452
6 Lederle, F.A., Wilson, S.E., Johnson, G.R., Reinke, D.B., Littooy, F.N., Acher, C.W. et al. (2002) Immediate repair compared with surveillance of small abdominal aortic aneurysms. *N. Engl. J. Med.* **346**, 1437–1444
7 Cao, P., De Rango, P., Verzini, F., Parlani, G., Romano, L., Cieri, E. et al. (2011) Comparison of surveillance versus aortic endografting for small aneurysm repair (CAESAR): results from a randomised trial. *Eur. J. Vasc. Endovasc. Surg.* **41**, 13–25
8 Ouriel, K., Clair, D.G., Kent, K.C., Zarins, C.K. and Positive Impact of Endovascular Options for treating Aneurysms Early (PIVOTAL) Investigators (2010) Endovascular repair compared with surveillance for patients with small abdominal aortic aneurysms. *J. Vasc. Surg.* **51**, 1081–1087
9 Golledge, J., Norman, P.E., Murphy, M.P. and Dalman, R.L. (2016) Challenges and opportunities in limiting abdominal aortic aneurysm growth. *J. Vasc. Surg.* **65**, 225–233
10 Golledge, J. and Norman, P.E. (2011) Current status of medical management for abdominal aortic aneurysm. *Atherosclerosis* **217**, 57–63
11 Krishna, S.M. and Golledge, J. (2013) The role of thrombospondin-1 in cardiovascular health and pathology. *Int. J. Cardiol.* **168**, 692–706
12 Bornstein, P. (2001) Thrombospondins as matricellular modulators of cell function. *J. Clin. Invest.* **107**, 929–934
13 Esemuede, N., Lee, T., Pierre-Paul, D., Sumpio, B.E. and Gahtan, V. (2004) The role of thrombospondin-1 in human disease. *J. Surg. Res.* **122**, 135–142
14 Xia, Y., Dobaczewski, M., Gonzalez-Quesada, C., Chen, W., Biernacka, A., Li, N. et al. (2011) Endogenous thrombospondin 1 protects the pressure-overloaded myocardium by modulating fibroblast phenotype and matrix metabolism. *Hypertension* **58**, 902–911
15 Lee, T., Esemuede, N., Sumpio, B.E. and Gahtan, V. (2003) Thrombospondin-1 induces matrix metalloproteinase-2 activation in vascular smooth muscle cells. *J. Vasc. Surg.* **38**, 147–154
16 Chen, D., Asahara, T., Krasinski, K., Witzenbichler, B., Yang, J., Magner, M. et al. (1999) Antibody blockade of thrombospondin accelerates reendothelialization and reduces neointima formation in balloon-injured rat carotid artery. *Circulation* **100**, 849–854
17 Roth, J.J., Gahtan, V., Brown, J.L., Gerhard, C., Swami, V.K., Rothman, V.L. et al. (1998) Thrombospondin-1 is elevated with both intimal hyperplasia and hypercholesterolemia. *J. Surg. Res.* **74**, 11–16
18 Reed, M.J., Iruela-Arispe, L., O'Brien, E.R., Truong, T., LaBell, T., Bornstein, P. et al. (1995) Expression of thrombospondins by endothelial cells. Injury is correlated with TSP-1. *Am J Pathol.* **147**, 1068–1080
19 Maier, K.G., Han, X., Sadowitz, B., Gentile, K.L., Middleton, F.A. and Gahtan, V. (2010) Thrombospondin-1: a proatherosclerotic protein augmented by hyperglycemia. *J. Vasc. Surg.* **51**, 1238–1247

20 Schellings, M.W., van Almen, G.C., Sage, E.H. and Heymans, S. (2009) Thrombospondins in the heart: potential functions in cardiac remodeling. *J. Cell Commun. Signal.* **3**, 201–213
21 Frangogiannis, N.G., Ren, G., Dewald, O., Zymek, P., Haudek, S., Koerting, A. et al. (2005) Critical role of endogenous thrombospondin-1 in preventing expansion of healing myocardial infarcts. *Circulation* **111**, 2935–2942
22 Raman, P., Krukovets, I., Marinic, T.E., Bornstein, P. and Stenina, O.I. (2007) Glycosylation mediates up-regulation of a potent antiangiogenic and proatherogenic protein, thrombospondin-1, by glucose in vascular smooth muscle cells. *J. Biol. Chem.* **282**, 5704–5714
23 Moxon, J.V., Padula, M.P., Clancy, P., Emeto, T.I., Herbert, B.R., Norman, P.E. et al. (2011) Proteomic analysis of intra-arterial thrombus secretions reveals a negative association of clusterin and thrombospondin-1 with abdominal aortic aneurysm. *Atherosclerosis* **219**, 432–439
24 Krishna, S.M., Seto, S.W., Jose, R.J., Biros, E., Moran, C.S., Wang, Y. et al. (2015) A peptide antagonist of thrombospondin-1 promotes abdominal aortic aneurysm progression in the angiotensin II-infused apolipoprotein-E-deficient mouse. *Arterioscler. Thromb. Vasc. Biol.* **35**, 389–398
25 Chen, X., Rateri, D.L., Howatt, D.A., Balakrishnan, A., Moorleghen, J.J., Cassis, L.A. et al. (2016) TGF-β neutralization enhances AngII-induced aortic rupture and aneurysm in both thoracic and abdominal regions. *PLoS ONE* **11**, e0153811
26 Liu, Z., Morgan, S., Ren, J., Wang, Q., Annis, D.S., Mosher, D.F. et al. (2015) Thrombospondin-1 (TSP1) contributes to the development of vascular inflammation by regulating monocytic cell motility in mouse models of abdominal aortic aneurysm. *Circ. Res.* **117**, 129–141
27 Golledge, J. and Norman, P.E. (2010) Atherosclerosis and abdominal aortic aneurysm: cause, response, or common risk factors? *Arterioscler. Thromb. Vasc. Biol.* **30**, 1075–1077
28 Ng, T.F., Turpie, B. and Masli, S. (2009) Thrombospondin-1-mediated regulation of microglia activation after retinal injury. *Invest. Ophthalmol. Vis. Sci.* **50**, 5472–5478
29 Moura, R., Tjwa, M., Vandervoort, P., Van Kerckhoven, S., Holvoet, P. and Hoylaerts, M.F. (2008) Thrombospondin-1 deficiency accelerates atherosclerotic plaque maturation in ApoE-/- mice. *Circ. Res.* **103**, 1181–1189
30 Norman, P.E., Flicker, L., Almeida, O.P., Hankey, G.J., Hyde, Z. and Jamrozik, K. (2009) Cohort profile: the Health In Men Study (HIMS). *Int. J. Epidemiol.* **38**, 48–52
31 Golledge, J., Karan, M., Moran, C.S., Muller, J., Clancy, P., Dear, A.E. et al. (2008) Reduced expansion rate of abdominal aortic aneurysms in patients with diabetes may be related to aberrant monocyte-matrix interactions. *Eur. Heart. J.* **29**, 665–672
32 Norman, P., Spencer, C.A., Lawrence-Brown, M.M. and Jamrozik, K. (2004) C-reactive protein levels and the expansion of screen-detected abdominal aortic aneurysms in men. *Circulation* **110**, 862–866
33 Golledge, J., Muller, R., Clancy, P., McCann, M. and Norman, P.E. (2011) Evaluation of the diagnostic and prognostic value of plasma D-dimer for abdominal aortic aneurysm. *Eur. Heart. J.* **32**, 354–364
34 Golledge, J., Clancy, P., Moran, C., Biros, E., Rush, C., Walker, P. et al. (2010) The novel association of the chemokine CCL22 with abdominal aortic aneurysm. *Am. J. Pathol.* **176**, 2098–2106
35 Ferguson, C.D., Clancy, P., Bourke, B., Walker, P.J., Dear, A., Buckenham, T. et al. (2010) Association of statin prescription with small abdominal aortic aneurysm progression. *Am. Heart. J.* **159**, 307–313
36 Golledge, J., Muller, J., Shephard, N., Clancy, P., Smallwood, L., Moran, C. et al. (2007) Association between osteopontin and human abdominal aortic aneurysm. *Arterioscler. Thromb. Vasc. Biol.* **27**, 655–660
37 Rush, C., Nyara, M., Moxon, J.V., Trollope, A, Cullen, B and Golledge, J. (2009) Whole genome expression analysis within the angiotensin II-apolipoprotein E deficient mouse model of abdominal aortic aneurysm. *BMC Genomics* **10**, 298
38 Krishna, S.M., Seto, S.W., Moxon, J.V., Rush, C., Walker, P.J., Norman, P.E. et al. (2012) Fenofibrate increases high-density lipoprotein and sphingosine 1 phosphate concentrations limiting abdominal aortic aneurysm progression in a mouse model. *Am. J. Pathol.* **181**, 706–718
39 Seto, S.W., Krishna, S.M., Moran, C.S., Liu, D. and Golledge, J. (2014) Aliskiren limits abdominal aortic aneurysm, ventricular hypertrophy and atherosclerosis in an apolipoprotein E deficient mouse model. *Clin. Sci. (Lond.)* **127**, 123–134
40 Moran, C.S., Jose, R.J., Moxon, J.V., Roomberg, A., Norman, P.E., Rush, C. et al. (2013) Everolimus limits aortic aneurysm in the apolipoprotein E-deficient mouse by downregulating C-C chemokine receptor 2 positive monocytes. *Arterioscler. Thromb. Vasc. Biol.* **33**, 814–821
41 Moran, C.S., Jose, R.J., Biros, E. and Golledge, J. (2014) Osteoprotegerin deficiency limits angiotensin II-Induced aortic dilatation and rupture in the apolipoprotein E-knockout mouse. *Arterioscler. Thromb. Vasc. Biol.* **34**, 2609–2616
42 Seto, S.W., Krishna, S.M., Yu, H., Liu, D., Khosla, S. and Golledge, J. (2013) Impaired acetylcholine-induced endothelium-dependent aortic relaxation by caveolin-1 in angiotensin II-infused apolipoprotein-E (ApoE-/-) knockout mice. *PLoS ONE* **8**, e58481
43 Golledge, J., Leicht, A., Crowther, R.G., Clancy, P., Spinks, W.L. and Quigley, F. (2007) Association of obesity and metabolic syndrome with the severity and outcome of intermittent claudication. *J. Vasc. Surg.* **45**, 40–46
44 Golledge, J., Jayalath, R., Oliver, L., Parr, A., Schurgers, L. and Clancy, P. (2008) Relationship between CT anthropometric measurements, adipokines and abdominal aortic calcification. *Atherosclerosis* **197**, 428–434
45 Golledge, J., Jones, L., Oliver, L., Quigley, F. and Karan, M. (2006) Folic acid, vitamin B12, MTHFR genotypes, and plasma homocysteine. *Clin. Chem.* **52**, 1205–1206
46 Smallwood, L., Allcock, R., van Bockxmeer, F., Warrington, N., Palmer, L.J., Iacopetta, B. et al. (2008) Polymorphisms of the matrix metalloproteinase 9 gene and abdominal aortic aneurysm. *Br. J. Surg.* **95**, 1239–1244
47 Collins, A.R., Meehan, W.P., Kintscher, U., Jackson, S., Wakino, S., Noh, G. et al. (2001) Troglitazone inhibits formation of early atherosclerotic lesions in diabetic and nondiabetic low density lipoprotein receptor-deficient mice. *Arterioscler. Thromb. Vasc. Biol.* **21**, 365–371
48 Wang, Y.X., Martin-McNulty, B., da Cunha, V., Vincelette, J., Lu, X., Feng, Q. et al. (2005) Fasudil, a Rho-kinase inhibitor, attenuates angiotensin II-induced abdominal aortic aneurysm in apolipoprotein E-deficient mice by inhibiting apoptosis and proteolysis. *Circulation* **111**, 2219–2226
49 Helske, S., Syvaranta, S., Kupari, M., Lappalainen, J., Laine, M., Lommi, J. et al. (2006) Possible role for mast cell-derived cathepsin G in the adverse remodelling of stenotic aortic valves. *Eur. Heart J.* **27**, 1495–1504

Clinical Science (2017) **131** 1261–1281
DOI: 10.1042/CS20160970

50 Wang, Y, Krishna, S.M., Moxon, J., Dinh, T.N., Jose, R.J., Yu, H. et al. (2014) Influence of apolipoprotein E, age and aortic site on calcium phosphate induced abdominal aortic aneurysm in mice. *Atherosclerosis* **235**, 204–212
51 Skelly, C.L., Chandiwal, A., Vosicky, J.E., Weichselbaum, R.R. and Roizman, B. (2007) Attenuated herpes simplex virus 1 blocks arterial apoptosis and intimal hyperplasia induced by balloon angioplasty and reduced blood flow. *Proc. Natl. Acad. Sci. U.S.A.* **104**, 12474–12478
52 Crossman, D.J., Ruygrok, P.N., Soeller, C. and Cannell, M.B. (2011) Changes in the organization of excitation-contraction coupling structures in failing human heart. *PLoS ONE* **6**, e17901
53 Ray, J.L., Leach, R., Herbert, J.M. and Benson, M. (2001) Isolation of vascular smooth muscle cells from a single murine aorta. *Methods Cell Sci.* **23**, 185–188
54 Cassis, L.A., Gupte, M., Thayer, S., Zhang, X., Charnigo, R., Howatt, D.A. et al. (2009) ANG II infusion promotes abdominal aortic aneurysms independent of increased blood pressure in hypercholesterolemic mice. *Am. J. Physiol. Heart Circ. Physiol.* **296**, H1660–H1665
55 Wang, L., Murphy-Ullrich, J.E. and Song, Y. (2014) Molecular insight into the effect of lipid bilayer environments on thrombospondin-1 and calreticulin interactions. *Biochemistry* **53**, 6309–6322
56 Pallero, M.A., Elzie, C.A., Chen, J., Mosher, D.F. and Murphy-Ullrich, J.E. (2008) Thrombospondin 1 binding to calreticulin-LRP1 signals resistance to anoikis. *FASEB J.* **22**, 3968–3979
57 Golledge, J. and Kuivaniemi, H. (2013) Genetics of abdominal aortic aneurysm. *Curr. Opin. Cardiol.* **28**, 290–296
58 Zhao, Y., Xiong, Z., Lechner, E.J., Klenotic, P.A., Hamburg, B.J., Hulver, M. et al. (2014) Thrombospondin-1 triggers macrophage IL-10 production and promotes resolution of experimental lung injury. *Mucosal Immunol.* **7**, 440–448
59 Weiss, D., Kools, J.J. and Taylor, W.R. (2001) Angiotensin II-induced hypertension accelerates the development of atherosclerosis in apoE-deficient mice. *Circulation* **103**, 448–454
60 Su, E.J., Lombardi, D.M., Siegal, J. and Schwartz, S.M. (1998) Angiotensin II induces vascular smooth muscle cell replication independent of blood pressure. *Hypertension* **31**, 1331–1337
61 Isenberg, J.S., Qin, Y., Maxhimer, J.B., Sipes, J.M., Despres, D., Schnermann, J. et al. (2009) Thrombospondin-1 and CD47 regulate blood pressure and cardiac responses to vasoactive stress. *Matrix Biol.* **28**, 110–119
62 Kuivaniemi, H., Platsoucas, C.D. and Tilson, III, M.D. (2008) Aortic aneurysms: an immune disease with a strong genetic component. *Circulation* **117**, 242–252
63 Koch, AE, Haines, G.K., Rizzo, R.J., Radosevich, J.A., Pope, R.M., Robinson, P.G. et al. (1990) Human abdominal aortic aneurysms. Immunophenotypic analysis uggesting an immune-mediated responses. *Am. J. Pathol.* **137**, 1199–1213
64 Doyen, V., Rubio, M., Braun, D., Nakajima, T., Abe, J., Saito, H. et al. (2003) Thrombospondin 1 is an autocrine negative regulator of human dendritic cell activation. *J. Exp. Med.* **198**, 1277–1283
65 Varma, V., Yao-Borengasser, A., Bodles, A.M., Rasouli, N., Phanavanh, B., Nolen, G.T. et al. (2008) Thrombospondin-1 is an adipokine associated with obesity, adipose inflammation, and insulin resistance. *Diabetes* **57**, 432–439
66 Lawler, J., Sunday, M., Thibert, V., Duquette, M., George, E.L., Rayburn, H. et al. (1998) Thrombospondin-1 is required for normal murine pulmonary homeostasis and its absence causes pneumonia. *J. Clin. Invest.* **101**, 982–992
67 Crawford, S.E., Stellmach, V., Murphy-Ullrich, J.E., Ribeiro, S.M., Lawler, J., Hynes, R.O. et al. (1998) Thrombospondin-1 is a major activator of TGF-beta1 *in vivo*. *Cell* **93**, 1159–1170
68 Saraff, K., Babamusta, F., Cassis, L.A. and Daugherty, A. (2003) Aortic dissection precedes formation of aneurysms and atherosclerosis in angiotensin II-infused, apolipoprotein E-deficient mice. *Arterioscler. Thromb. Vasc. Biol.* **23**, 1621–1626
69 Powell, J.T. and Brady, A.R. (2004) Detection, management, and prospects for the medical treatment of small abdominal aortic aneurysms. *Arterioscler. Thromb. Vasc. Biol.* **24**, 241–245
70 Jacob, T., Ascher, E., Hingorani, A., Gunduz, Y. and Kallakuri, S. (2001) Initial steps in the unifying theory of the pathogenesis of artery aneurysms. *J. Surg. Res.* **101**, 37–43
71 Savill, J., Hogg, N., Ren, Y. and Haslett, C. (1992) Thrombospondin cooperates with CD36 and the vitronectin receptor in macrophage recognition of neutrophils undergoing apoptosis. *J. Clin. Invest.* **90**, 1513–1522
72 Stern, M., Savill, J. and Haslett, C. (1996) Human monocyte-derived macrophage phagocytosis of senescent eosinophils undergoing apoptosis. Mediation by alpha v beta 3/CD36/thrombospondin recognition mechanism and lack of phlogistic response. *Am. J. Pathol.* **149**, 911–921
73 Wilson, W.R., Anderton, M., Schwalbe, E.C., Jones, J.L., Furness, P.N., Bell, P.R. et al. (2006) Matrix metalloproteinase-8 and -9 are increased at the site of abdominal aortic aneurysm rupture. *Circulation* **113**, 438–445
74 Maclauchlan, S., Skokos, E.A., Agah, A., Zeng, J., Tian, W., Davidson, J.M. et al. (2009) Enhanced angiogenesis and reduced contraction in thrombospondin-2-null wounds is associated with increased levels of matrix metalloproteinases-2 and -9, and soluble VEGF. *J. Histochem. Cytochem.* **57**, 301–313
75 Schroen, B., Heymans, S., Sharma, U., Blankesteijn, W.M., Pokharel, S., Cleutjens, J.P. et al. (2004) Thrombospondin-2 is essential for myocardial matrix integrity: increased expression identifies failure-prone cardiac hypertrophy. *Circ. Res.* **95**, 515–522
76 Rodriguez-Manzaneque, J.C., Lane, T.F., Ortega, M.A., Hynes, R.O., Lawler, J. and Iruela-Arispe, M.L. (2001) Thrombospondin-1 suppresses spontaneous tumor growth and inhibits activation of matrix metalloproteinase-9 and mobilization of vascular endothelial growth factor. *Proc. Natl. Acad. Sci. U.S.A.* **98**, 12485–12490
77 Taraboletti, G., Morbidelli, L., Donnini, S., Parenti, A., Granger, H.J., Giavazzi, R. et al. (2000) The heparin binding 25 kDa fragment of thrombospondin-1 promotes angiogenesis and modulates gelatinase and TIMP-2 production in endothelial cells. *FASEB J.* **14**, 1674–1676
78 Thompson, R.W., Holmes, D.R., Mertens, R.A., Liao, S., Botney, M.D., Mecham, R.P. et al. (1995) Production and localization of 92-kilodalton gelatinase in abdominal aortic aneurysms. An elastolytic metalloproteinase expressed by aneurysm-infiltrating macrophages. *J Clin Invest.* **96**, 318–326

79 Lindeman, J.H., Ashcroft, B.A., Beenakker, J.W., van Es, M., Koekkoek, N.B., Prins, F.A. et al. (2010) Distinct defects in collagen microarchitecture underlie vessel-wall failure in advanced abdominal aneurysms and aneurysms in Marfan syndrome. *Proc. Natl. Acad. Sci. U.S.A.* **107**, 862–865
80 Vande Geest, J.P., Sacks, M.S. and Vorp, D.A. (2006) The effects of aneurysm on the biaxial mechanical behavior of human abdominal aorta. *J. Biomech.* **39**, 1324–1334
81 Wilson, K.A., Lindholt, J.S., Hoskins, P.R., Heickendorff, L., Vammen, S. and Bradbury, A.W. (2001) The relationship between abdominal aortic aneurysm distensibility and serum markers of elastin and collagen metabolism. *Eur. J. Vasc. Endovasc. Surg.* **21**, 175–178
82 Choke, E., Cockerill, G., Wilson, W.R., Sayed, S., Dawson, J., Loftus, I. et al. (2005) A review of biological factors implicated in abdominal aortic aneurysm rupture. *Eur. J. Vasc. Endovasc. Surg.* **30**, 227–244
83 Carmo, M., Colombo, L., Bruno, A., Corsi, F.R., Roncoroni, L., Cuttin, M.S. et al. (2002) Alteration of elastin, collagen and their cross-links in abdominal aortic aneurysms. *Eur. J. Vasc. Endovasc. Surg.* **23**, 543–549
84 Treska, V. and Topolcan, O. (2000) Plasma and tissue levels of collagen types I and III markers in patients with abdominal aortic aneurysms. *Int. Angiol.* **19**, 64–68
85 Deak, S.B., Ricotta, J.J., Mariani, T.J., Deak, S.T., Zatina, M.A., Mackenzie, J.W. et al. (1992) Abnormalities in the biosynthesis of type III procollagen in cultured skin fibroblasts from two patients with multiple aneurysms. *Matrix* **12**, 92–100
86 Kuga, T., Esato, K., Zempo, N., Fujioka, K. and Nakamura, K. (1998) Detection of type III collagen fragments in specimens of abdominal aortic aneurysms. *Surg. Today* **28**, 385–390
87 Muratoglu, S.C., Belgrave, S., Hampton, B., Migliorini, M., Coksaygan, T., Chen, L. et al. (2013) LRP1 protects the vasculature by regulating levels of connective tissue growth factor and HtrA1. *Arterioscler. Thromb. Vasc. Biol.* **33**, 2137–2146
88 Gorovoy, M., Gaultier, A., Campana, W.M., Firestein, G.S. and Gonias, S.L. (2010) Inflammatory mediators promote production of shed LRP1/CD91, which regulates cell signaling and cytokine expression by macrophages. *J. Leukoc. Biol.* **88**, 769–778
89 Bown, M.J., Jones, G.T., Harrison, S.C., Wright, B.J., Bumpstead, S., Baas, A.F. et al. (2011) Abdominal aortic aneurysm is associated with a variant in low-density lipoprotein receptor-related protein 1. *Am. J. Hum. Genet.* **89**, 619–627
90 Galora, S., Saracini, C., Pratesi, G., Sticchi, E., Pulli, R., Pratesi, C. et al. (2015) Association of rs1466535 LRP1 but not rs3019885 SLC30A8 and rs6674171 TDRD10 gene polymorphisms with abdominal aortic aneurysm in Italian patients. *J. Vasc. Surg.* **61**, 787–792
91 Moxon, J.V., Behl-Gilhotra, R., Morton, S.K., Krishna, S.M., Seto, S.W., Biros, E. et al. (2015) Plasma low-density lipoprotein receptor-related protein 1 concentration is not associated with human abdominal aortic aneurysm presence. *Eur. J. Vasc. Endovasc. Surg.* **50**, 466–473
92 Mofidi, R., Goldie, V.J., Kelman, J., Dawson, A.R., Murie, J.A. and Chalmers, R.T. (2007) Influence of sex on expansion rate of abdominal aortic aneurysms. *Br. J. Surg.* **94**, 310–314